Thickness Dependence of κ_2 and Related Problems for Superconducting Alloy Films in Strong Fields

E. GUYON* AND F. MEUNIER
Faculté des Sciences, Laboratoire de Physique des Solides associé au Centre National de la Recherche Scientifique, Orsay, France

AND

R. S. THOMPSON†
Service de Physique Théorique, Centre d'Etudes Nucléaires de Saclay Gif-sur-Yvette, Saclay, France

(Received 23 August 1966)

Using the tunneling technique, we have studied superconducting alloy films of InBi in strong magnetic fields parallel and perpendicular to the surface. Measurements in perpendicular geometry confirm previous results for bulk type-II samples. Additionally they show the decreased effect of screening currents for thin films predicted by Maki. In parallel geometry we find the parameter κ_2 (related to the slope of the magnetization in high field) to be a function of film thickness. Anomalies observed from tunneling characteristics which we associated with the entry of flux quanta in the film are studied in detail. We construct a general diagram showing the film behavior near the nucleation field as a function of thickness and Ginzburg-Landau parameter κ.

I. INTRODUCTION

THE phenomenological theory of Ginzburg and Landau[1] [GL], which was later derived from the microscopic BCS theory[2] by Gor'kov[3] for superconductors near their transition temperature, has proved enormously useful for understanding the effects of strong magnetic fields on superconductivity. This theory was used by Abrikosov[4] to show the vortex nature of type-II superconductors, and by Saint James and de Gennes[5] to predict surface superconductivity. Then Maki[6] and de Gennes[7] extended the GL theory to all temperatures for dirty alloys when the field is near its critical value. In particular, Maki extended the GL parameter κ to all temperatures as two functions: (a) κ_1 related to the value of the upper critical field, and (b) κ_2 related to the magnetization in high field. Experimentally, κ_1 was observed to increase as the temperature was lowered, as was predicted by Maki. Furthermore, κ_2 was seen to increase like κ_1.[8] Maki had predicted a decreasing κ_2. Subsequently, Caroli, Cyrot, and de Gennes[9] showed that κ_2 should nearly equal κ_1 for a bulk type-II superconductor. However, Baratoff[10] then noted that the κ_2 appropriate to a thin film in a magnetic field parallel to its surface should be the decreasing function originally calculated by Maki.

The present work was started to find experimentally and theoretically whether or not different κ_2's apply and to explain the cause of such a discrepancy. Experimentally the very small magnetization of a thin film is difficult to measure. However, both the magnetization and the amplitude of the deviation of the density of electronic states from that of a normal metal are proportional to the square of the magnitude of the order parameter near the upper critical field H_M: They go to zero continuously when $H = H_M$, as expected from the fact that the transition is second order in the magnetic field. Therefore we can obtain the desired information by using the tunneling technique.[11] Tunneling characteristics of InBi alloy films of 2 to 3 atomic % Bi have been measured for thicknesses ranging from 200 to 10 000 Å. The ratio of the residual mean free path in the normal phase l to the BCS coherence length ξ_0 for these alloys is $l/\xi_0 \sim \frac{1}{10}$. Corrections to the dirty limit, where the ratio is zero, are not negligible. Therefore, in addition to calculating the tunneling characteristics for all film thicknesses, we have studied the approximate corrections for small departures from the dirty limit. Experimental results for pure In films are given but not discussed quantitatively owing to the lack of a complete theoretical treatment. Moreover, possible thickness modulation and the precise nature of electron scattering at the boundaries, which are not easily controlled, should play a much more important role for pure films[12] than for the dirty ones on which we focus our attention.

* Present address: Department of Physics, University of California, Los Angeles, California.

† National Science Foundation. Postdoctoral Fellow. Present address: Institute for Physical Problems of the Academy of Sciences of the USSR, Vorobyevskoye Shosse 2, Moscow B-334.

[1] V. L. Ginzburg and L. D. Landau, Zh. Eksperim. i Teor. Fiz. **20**, 1064 (1950).

[2] J. Bardeen, L. N. Cooper, and J. R. Schrieffer, Phys. Rev. **108**, 1175 (1957).

[3] L. P. Gorkov, Zh. Eksperim. i Teor. Fiz. **36**, 1918 (1959); **37**, 1402 (1959) [English transls.: Soviet Phys.—JETP **9**, 1364 (1959); **10**, 998 (1960)].

[4] A. A. Abrikosov, J. Phys. Chem. Solids **2**, 199 (1957).

[5] D. Saint James and P. G. De Gennes, Phys. Letters **9**, 217 (1964).

[6] K. Maki, Physics **1**, 21 (1964).

[7] P. G. De Gennes, Phys. Kondensierten Materie **3**, 79 (1964).

[8] T. McConville and P. Serin, Phys. Rev. **140**, A1169 (1965); G. Bon Mardion, B. B. Goodman, and A. Lacaze, J. Phys. Chem. Solids **26**, 1143 (1965).

[9] C. Caroli, M. Cyrot and P. G. De Gennes, Solid State Commun. **4**, 17 (1966).

[10] A. Baratoff, Bull. Am. Phys. Soc. **11**, 175 (1966); R. S. Thompson and A. Baratoff (to be published).

[11] (a) E. Guyon, J. Matricon, A. Martinet, and P. Pincus, Phys. Rev. **138**, A746 (1965); (b) E. Guyon, Advan. Phys. **15**, 417 (1966).

[12] P. G. De Gennes and M. Tinkham, Physics **1**, 107 (1964).

Our experimental techniques are described in the following section. Section III is devoted to a general discussion of the extended GL theory as it applies to thick or thin films in parallel or perpendicular fields. Expressions for the tunneling characteristics are given, and the difference between the different forms of κ_2 is explained to arise from the spatial variations of the magnitude of the order parameter. More detailed calculations are found in two appendices. Experimental results are compared with theory for perpendicular fields in Sec. IV, for thin films in parallel fields in Sec. V, and for thicker films in parallel fields in Sec. VI. A diagram giving the type of transition to the normal state and character of the superconductivity near the critical field as a function of thickness and κ value is presented and discussed in Sec. VII.

II. EXPERIMENTAL TECHNIQUES

The technical part of our experiments has already been described.[11] We may recall its general features and present the new aspects related to the use of these films.

(*A*) *The films* were evaporated from a Joule-heated crucible under a vacuum of less than 10^{-6} Torr in a conventional evaporator. The substrates were microscopic slides ($\frac{1}{10}$-mm thick) glued with GE7031 varnish on copper plates. The plates were coupled by copper tresses to a container which could be filled from the outside with liquid nitrogen. The temperature of the films could be kept to -170°C during the evaporation.

A thin (200 Å) film of Al[13] was deposited on a first layer of SiO and then oxydized by a glow discharge under a reduced pressure of dry O_2. Then we evaporated the **In**Bi film from a piece of bulk ingot in a single crucible on the cooled substrate.

This procedure has given **In**Bi films of a remarkable thickness homogeneity. The relative thickness modulation for 200 Å films was less than 5% except at the edges. Such films were continuous resistivity and the thickness deduced from room-temperature resistance agreed with the optical measurements. Such a behavior is to be compared with that of films evaporated on room-temperature substrates. A 200 Å **In**Bi film prepared under otherwise similar conditions is not continuous resistively. It looks gray and is transparent. The low-temperature thinner films develop the same properties after several days at room temperature. An electron-microscope study was performed in these two cases. The **In**Bi films were evaporated on a soluble substrate on top of a first layer of SiO (just as for the films studied on the microscope slides). The films evaporated at low temperature are continuous and composed of small grains of average size 500 Å, randomly orientated. Those evaporated at room temperature have large, well crystallized, and isolated grains.

[13] The Al film was in the normal state in our experiments performed at $T>1.2$°K.

The critical process for this recrystallization which gives the "poor" films has to occur during or immediately after the evaporation. Just at the condensation, the crystallization is mainly caused by the surface mobility, which is low for N_2-temperature films. Moreover, the continuous films so obtained may be stabilized later by the superficial films (oxide, adsorbed gases) formed on them.

Properties of the thicker films evaporated at low temperature agreed with those of the bulk materials.

(*B*) *Tunneling measurements:* Films were placed in a bath of He^4 which could be pumped down to 1.2°K. We recorded the differential conductance $dI(V)/dV$ of the junction with a system developed in Orsay[14] using a synchronous detection. The accuracy of 1% to 5% depended very much on the noise of the junction. Our results are presented in terms of a normalized differential conductance

$$D(V)=\frac{1}{C_n}\frac{dI(V)}{dV}, \tag{2.1}$$

where C_n is the measured conductance in the normal state.

(*C*) *A Magnetic field* could be applied at different angles to the films with a 15-kG electromagnet. In order to study the dependence on field of the differential conductance, we set $V=0$ and recorded $D_{V=0}(H)$.[15] The maximum or upper critical field H_M is given by $D_{V=0}(H_M)=1$. This procedure allows a very accurate determination of H_M since $D(H)$ varies linearly for a large range of the subcritical field. A typical curve (Fig. 3, upper curve) shows the "tail effects" due to the continuous edges; the extrapolation of the linear part of the curve near $D\ (V=0)=1$ gives $H_{||}$ with a 1% accuracy. ($H_{||}$ is H_M for a field parallel to the junction.)

The slope S of $D_{V=0}(H)$ in the linear region is defined as

$$S=(1-D_{V=0}(H))/(H_M-H). \tag{2.2}$$

Usually we measure $1-D_{V=0}(H)$ for $H_M-H=100$ G so that we obtain numerically $100S$.

The value of the field H_M is very sensitive to the orientation of the field; the alignment could be done with an accuracy of $\pm 15'$. This actually limits the accuracy of the determination of the upper critical field in parallel geometry for the thinnest films. The accuracy of S is only 5% owing to the necessity of normalization for $D(V)$.

(*D*) *The critical temperature* T_c could be taken from resistive measurements. The edges, which were continuous resistively because of the low-temperature evaporation, had been trimmed. However we prefer to take T_c from the temperature variation of $H_{||}$ (near T_c,

[14] A. Gaudefroy, E. Guyon, A. Martinet, and J. Sanchez, Rev. Phys. Appl. 1, 18 (1966).

[15] The choice of $V=0$ is not restrictive since in the gapless regime the $D(V)$ curve simply decreases by a uniform multiple as the field is increased.

$H_{||}^2\alpha[T-T_c]$). A very accurate determination is thus obtained on the junction itself. Moreover, the T_c of very thin films depends on the strains developed in cooling and may be different on the different substrates (Al_2O_3 for the junctions, SiO for measuring resistive transitions).

(*E*) *Thickness* was measured optically by an interferometric method. The absolute accuracy, typically ± 100 Å, is very poor for the thinnest films. The resistance measurement seems to give accurate results in this case but, in fact, the resistivity may become dependent on structure and thickness. Actually the thickness was taken directly from the critical-field data (Sec. V A).

(*F*) *Resistivity:* From the previous discussion one sees that a direct measurement of the residual resistivity ρ_R is inaccurate. We usually measure the resistivity ratio r_R and obtain ρ_R from the Matthiesen rule $(\rho_0+\rho_R)/\rho_R=r_R$. (We used the room-temperature resistivity for pure In: $\rho_0=9\ \mu\Omega$ cm.) Such a method gives good results in the case of thick films where its use can be controlled. However we rather use directly the transport properties obtained in the superconducting state.

(*G*) *The product* $\rho_R l$ where l[16] is the residual mean free path is nearly constant for different alloys. Its value indirectly gives l, which always enters with ξ_0 into the properties of dirty materials. However, there is a large scatter in the published data for In, which may be due in part to the different techniques used: anomalous skin effect on bulk samples,[17] and dc resistivity measurements on films.[18–20] We have used this last technique to get our own data on **In**Bi 0.2% in the case $l<d$. (The extrapolation of the linear part of the $\rho_R d$-versus-d diagram to $d=0$ gives $\frac{3}{8}\rho_R l$ if we assume a diffuse scattering at the boundaries.) Our results give

$$\rho_R l=(1.1\pm 0.1)\times 10^{-11}\ \Omega\ \text{cm}.$$

They agree with the most recent and similar measurements by Chaudhari and Brown.[20]

(*H*) *The Ginzburg-Landau parameter* κ was determined from the limiting form

$$\frac{(dH_{c2}/dT)_{T_c}}{(dH_{cB}/dT)_{T_c}}=\kappa\sqrt{2}.$$

H_{c2} ($=H_M$ for a thick film in perpendicular field) varies linearly with T on a large domain ($0.7<t<1$). The slope at T_c of the bulk critical field H_{cB} was taken from Kinsel's[21] results. One obtains nearly $(dH_{cB}/dT)_{T=T_c}=40T_c+12$ for a Bi concentration from 0 to 3%.

[16] l is the bulk mean free path. We use later l_{eff} for the mean free path which takes into account the effect of the boundaries.

[17] P. N. Dheer, Proc. Roy. Soc. (London) **A260**, 333 (1961).

[18] A. M. Toxen, Phys. Rev. **123**, 442 (1961); **127**, 382 (1962); A. M. Toxen and M. J. Burns, *ibid.* **130**, 1808 (1963).

[19] A. M. Toxen, J. J. Burns, and D. J. Quinn, Phys. Rev. **138**, A1145 (1965).

[20] R. D. Chaudhari and J. B. Brown, Phys. Rev. **139**, A1482 (1965).

[21] T. Kinsel, thesis, Rutgers University, 1965 (unpublished).

III. THE GENERALIZED GINZBURG-LANDAU EQUATIONS AND GAPLESS SUPERCONDUCTIVITY

We use the results of the generalized GL equations in three sections, where we study: (A) the value of the upper critical fields H_M, (B) the universal form of the density of electronic states in the subcritical domain, (C) the amplitude of the deviation of the density of states (or the magnetization) from the normal-state value when the field varies. These properties have been studied rather thoroughly[8,11] for bulk type-II superconductors in high field and are generally associated, respectively, with notions of (A) $\kappa_1(t)$, (B) gapless superconductivity, (C) $\kappa_2(t)$. The same quantities may be studied in other geometries. In these three sections we will study the cases of: (1) a thin film in a perpendicular field (Abrikosov structure), (2) a thin film in a parallel field (constant order parameter), (3) a thicker film in a parallel field (surface superconductivity).

A. Upper Critical Field

In the presence of a magnetic field the condensed electrons experience an interaction acting with opposite signs on the two electrons of a Cooper pair, because of the $\mathbf{p}\cdot\mathbf{A}$ term of the interaction Hamiltonian ($\mathbf{p}$ is the canonical momentum, $\mathbf{A}$ the vector potential). In some sense this interaction breaks the pair and gives a finite lifetime τ_κ to the condensed electrons, where τ_κ is the eigenvalue[7] of the GL operator $(\nabla/i-\mathbf{A})^2$,[22] operating on the pair "wave function" or pair potential $\Delta(\mathbf{r})$:

$$(1/\tau_\kappa)\Delta(\mathbf{r})=D(\nabla/i-\mathbf{A})^2\Delta(\mathbf{r}). \tag{3.1}$$

[We ignore the interaction of the spin with the field, $\boldsymbol{\sigma}\cdot\mathbf{H}$. This is not a bad approximation since all fields of interest here are much less than the Pauli field ($\sim$5,000 G). The A^2 interaction is also small, since $|\mathbf{p}|\gg|\mathbf{A}|$.] Here D is the usual diffusion coefficient for normal electrons ($D=\frac{1}{3}v_F l$ for a spherical Fermi surface, v_F being the Fermi velocity). The diffusion equation (3.1) is expected to apply only in the case of dirty materials ($l\ll\xi_0$).[7] The characteristic distance ξ for changes in $\Delta(\mathbf{r})$ is obtained from (3.1),

$$\xi^2=D\tau_\kappa.$$

The decay process competes with a natural growth of pairs associated with[11b] a characteristic time $\tau(t)$, a universal function of the reduced temperature $t=T/T_c$:

$$1/\tau(t)=2\pi\rho T, \tag{3.2}$$

where ρ is obtained from

$$\ln t=\psi(1/2+\rho/2)-\psi(1/2)=\sum_{n=0}^{\infty}\frac{1}{n+\frac{1}{2}+\frac{1}{2}\rho}-\frac{1}{n+\frac{1}{2}}, \tag{3.3}$$

[22] We use $\hbar=k_B=2e/\hbar c=1$. The conversion factor for fields in gauss is just $2\pi/\Phi_0$ where Φ_0 is the flux quantum.

where ψ is the digamma function. An implicit expression for H_M is obtained by the condition that the two times compensate, i.e. $\tau(t)=\tau_\kappa$. We shall now evaluate the GL eigenvalue τ_κ in the three cases outlined above:

(1) The solution for the pair potential for a *film in a perpendicular field* is the same as for the vortex structure found by Abrikosov[4] for a bulk type-II superconductor. The eigenvalue of (3.1), found using a Gaussian wave function $\Delta=e^{-(1/2)Hx^2}$ (x is in the plane of the film) is

$$1/\tau_\kappa=DH. \tag{3.4}$$

The parameter $\kappa_1(t)$ is then defined as $H_\perp(t)/\sqrt{2}H_{cB}(t)$ where $H_\perp$ is H_M for perpendicular geometry. Good agreement has been obtained between the theoretical form of $\kappa_1(t)$ and experimental results.[11] For the thinnest films[16] $H_\perp$ becomes substantially larger than H_{c2} (see Sec. IV A). Then we call the parameter κ, κ_{eff}.

(2) For a *thin* $[d\ll\xi(t)]$ *film in a parallel field*, $|\Delta|$ is practically constant, and the eigenvalue (3.1) is obtained[23] by simply averaging $(\mathbf{A})^2$ over the width of the film d:

$$1/\tau_\kappa=DH^2d^2/12. \tag{3.5}$$

The square of the parallel upper critical field H^2 has the same temperature dependence as $H_\perp$ and may be written in terms of the same $\kappa_1(t)$,

$$\kappa_1(t)=H_{||}{}^2d^2/12\sqrt{2}H_{cB}.$$

(3) The eigenvalues for *thicker films in parallel fields* have been calculated by Saint James.[5] He plots the quantities $h=H_{||}(\frac{1}{2}d)^2$ versus $\epsilon=[d/2\xi(t)]^2=H_\perp(\frac{1}{2}d)^2$, which gives a universal relation between $H_{||}$ and $H_\perp$ *at all temperatures* in the dirty limit. The characteristics of the relation change very rapidly, at a critical value $\epsilon_{cr}=0.816$, from those of the thin films $[\epsilon=\frac{1}{3}h^2$ as seen from (3.4) and (3.5)] to those of the thick films having superconducting surface sheaths ($H_{c3}=1.7\ H_{c2}$ or $h=1.7\ \epsilon$). The sharp cusp which was observed in measurements of the angular dependence of H_M near the parallel orientation[24] exhibits the rapidity of the change of the solutions at ϵ_{cr}.

In the limit of a thick film $[d\gg\xi(t)]$, Δ is well represented by a sum of Gaussian functions centered at the boundaries[25]:

$$e^{-(\alpha H/2)(x-d/2)^2}+e^{-(\alpha H/2)(x+d/2)^2}$$

(film limited by $x=\pm d/2$).

The eigenvalue is

$$1/\tau_\kappa=\alpha DH, \tag{3.6}$$

where α equals 0.59. The exact result of Saint James and de Gennes, $H_{c3}=1.69H_{c2}$, is recovered to 2% accuracy.[11]

The thickness of the films and the value of $\xi(t)$ can be deduced from the values of $H_{||}$ and $H_\perp$ either by fitting the universal curve of Saint James[26] for thicker films or by using Eqs. (4) and (5) in the thin-film regime:

$$\xi^2(t)=(H_\perp)^{-1};$$
$$d^2=12H_\perp/(H_{||})^2.$$

However, for the films used here corrections must be applied to these simple formulas for the critical fields because of the finite value of l.

For "not too clean" films (small values of l/ξ_0) we may consider separately corrections of order l/ξ_0 and those of order l/d.

First we consider corrections arising from the *finite value of* l/ξ_0 ($\sim 1/7$). The corrections to the GL equations near T_c have been calculated for all values of l/ξ_0 by Gor'kov.[3] In the Pippard approximation it would suffice to replace all values of l in the above formulas by a coherence length $\xi=(\xi_0^{-1}+l^{-1})^{-1}\equiv l(1-l/\xi_0+\cdots)$. We discuss these corrections in more detail in Sec. IV, where we show that the results of Gor'kov give a slightly stronger correction $l\rightarrow l(1-1.4\ l/\xi_0)$ for the values of l/ξ_0 appropriate to our films.

The second class of corrections is due to the *finite ratio* l/d.

For perpendicular geometry these corrections arise from the diffuse scattering of electrons at the boundary. These corrections are the same as those which modify the conductivity[27] and may be calculated using the theory of Fuchs.[28] They increase the value of the critical field for thinner films, as we describe in Sec. IV.

For parallel geometry the corrections of order l/d arising from the boundary scattering must be considered simultaneously with the corrections of the same order arising from the nonlocal electrodynamics. One of us[29] has already calculated a function $f_D(l/d)$ which incorporates the combined effects. These corrections are large enough to change the dependence of $H_{||}$ on thickness from d^{-1} to $d^{-3/2}$ when $l\gg d$. In Sec. V we show explicitly how these corrections should be applied to deduce the values of d from knowledge of the critical fields.

In cleaner films all of the corrections must be considered simultaneously. This was done earlier[29] in the case of a thin film in a parallel field, where $l/\xi_0\simeq l/d\simeq 0.4$. The 10% deviations of the temperature dependence of H_M from that of formula (3.5) which were observed experimentally by Toxen[30] were explained. However, we are interested in seeing whether the limiting behavior of (3.5) is better attained for dirtier alloys, and we show in Sec. V that this is in fact the case.

[23] K. Maki, Progr. Theoret. Phys. (Kyoto) **31**, 731 (1964).
[24] D. Saint James, Phys. Letters **16**, 218 (1965); J. P. Burger, G. Deutscher, E. Guyon, and A. Martinet, *ibid.* **16**, 220 (1965).
[25] C. Kittel (private communication).
[26] J. P. Burger, G. Deutscher, E. Guyon, and A. Martinet, Phys. Rev. **137**, A853 (1965); G. Deutscher, thesis, Orsay, 1966 (unpublished).
[27] (a) E. Guyon, C. Caroli, and A. Martinet, J. Phys. (Paris) **25**, 683 (1964); (b) P. G. De Gennes, *Superconductivity of Metals and Alloys* (W. A. Benjamin, Inc., New York, 1966).
[28] K. Fuchs, Proc. Cambridge Phil. Soc. **34**, 100 (1938).
[29] R. S. Thompson and A. Baratoff, Phys. Rev. Letters **15**, 971 (1965); and to be published.
[30] A. M. Toxen, Rev. Mod. Phys. **36**, 308 (1964).

B. Gapless Superconductivity

A very spectacular feature of superconductors with $H \lesssim H_M$ is the absence of an energy gap in the excitation spectrum. The ratio of the density of states to that (N_0) of the normal metal is given in terms of the local value[7] of $|\Delta(\mathbf{r})|$:

$$\frac{N(E,\mathbf{r})}{N_0}=1+2|\Delta(\mathbf{r})|^2\tau^2\frac{(2E\tau)^2-1}{[(2E\tau)^2+1]^2}. \quad (3.7)$$

The energy E is measured from the Fermi level and τ is given by (3.2) and (3.3). Except for $|\Delta|^2$, the form of (3.7) is independent of the geometry and the "pair-breaking" mechanism. The energy scale of the anomalies of $N(E,\mathbf{r})$ is given by τ. The differential conductivity for tunneling of electrons across a voltage difference V is obtained[11] after integration of $N(E)$ over a Fermi distribution:

$$D(V)=\frac{1}{C_n}\frac{dI}{dV}=1+\frac{|\Delta|^2}{8\pi^2T^2}Re\psi_3\left[\frac{1}{2}+\frac{\rho}{2}+\frac{ieV}{2\pi T}\right], \quad (3.8)$$

where

$$\psi_3(Z)=\psi''(Z)=-\sum_{n=0}^{\infty}\frac{2}{(n+Z)^3},$$

and $|\Delta|^2$ is averaged over the surface of the film next to the junction.

In Fig. 1 we give tunneling measurements in the high field domain ($h=H/H_M \lesssim 1$) taken at 1.3°K for two samples having the same T_c and so the same τ. The $D(V)$ curves have been normalized to the same value at $V=0$ to show the shape of $D(V)-1$ independently of its magnitude.

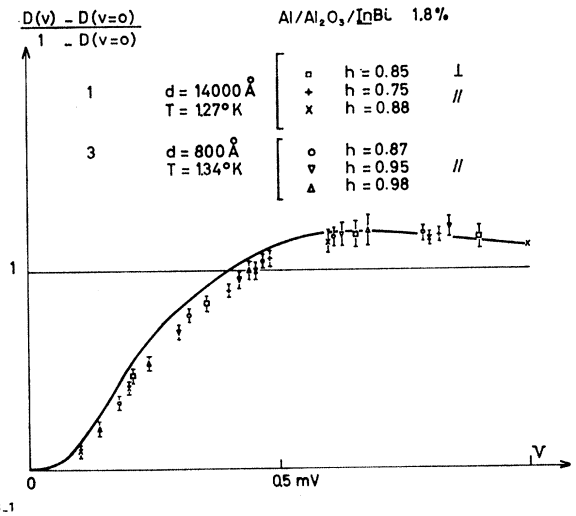

FIG. 1. Differential conductivity curves normalized at $V=0$, in high field ($h=H/H_m<1$). For the same T, these curves are the same for alloys of the same T_c, for any thickness, and any magnitude or orientation of the field. The continuous line is the theoretical curve.

All points are on the same curve regardless of the sample thickness and the value and orientation of the high fields, as expected theoretically. However the voltage where $D(V)=1$ is about 10% higher than expected from the theory.[31] This discrepancy may be due to the finite value of l/ξ_0 or to strong-coupling effects. In fact we find a zero-field gap $2\Delta_0=(3.9\pm0.1)T_c$ instead of the BCS value, $3.53T_c$. A similar and more important effect was found in the study of Pb alloys in the gapless region.[11] Such an effect would be important for the study of the detailed shape of $D(V)$. However, we will not take it into account, since our main interest is in amplitude effects which we assume can be studied independently.

C. Amplitude Effects in High Field

The correct generalized GL equation may be obtained following the work of Maki[6] and Caroli *et al.*[9]:

$$\left\{\sum_{n=0}^{\infty}\left(\frac{1}{n+\frac{1}{2}+\frac{1}{2}\rho}-\frac{1}{n+\frac{1}{2}}\right)-\ln t\right\}\Delta(\mathbf{r})=\frac{1}{8\pi^2T^2}$$
$$\times\sum_{n=0}^{\infty}\frac{1}{(n+\frac{1}{2}+\frac{1}{2}\rho)^4}\Delta(\mathbf{r})\left\{n+\frac{1}{2}-\frac{D}{4\pi T}\nabla^2\right\}|\Delta(\mathbf{r})|^2. \quad (3.9)$$

For $H=H_M$ the coefficient of the left-hand side of (3.9) equals zero and we obtain (3.3). Following the method of Abrikosov,[4] the magnitude of $|\Delta|^2$ is calculated as follows:

The solution is written as $\Delta(\mathbf{r})+\Delta_1(\mathbf{r})$ where $\Delta(\mathbf{r})$ is the solution of the linearized equation. Then (3.9) is multiplied by $\Delta^*(\mathbf{r})$ and integrated over the volume of the sample to eliminate by orthogonality Δ_1 and the necessity of considering changes in the form of Δ. The integral of the left-hand side is L, and that of the right-hand side R. Then two types of corrections to the linear ized equation appear: (a) those in R, (b) those arising from the difference between $\rho(H)$ and $\rho(H_M)$. First we consider the integral of the right-hand side:

$$R=\sum_{n=0}^{\infty}\frac{1}{8\pi^2T^2}\frac{1}{(n+\frac{1}{2}+\frac{1}{2}\rho)^4}\int dv|\Delta(\mathbf{r})|^2$$
$$\times\left\{n+\frac{1}{2}-\frac{D}{4\pi T}\nabla^2\right\}|\Delta(\mathbf{r})|^2, \quad (3.10)$$

which corresponds to the result obtained by Caroli, Cyrot, and de Gennes.[9] In general the κ_2 parameter is defined from R,

$$(\kappa_2)^2=\frac{3}{2}\frac{\lambda_L^2}{l^2}\frac{8\pi^2T^2}{(\psi_2)^2}\frac{R}{\int dv|\Delta(\mathbf{r})|^4}.$$

This choice of κ_2 is such that $\kappa_2(T_c)=\kappa_{GL}$. The difference between the function $\kappa_{2M}(t)$ defined by Maki,[6]

[31] Tinkham (private communication) has obtained a similar deviation for tunneling experiments on dirty Sn films.

which decreases with lowering of t, and the increasing function $\kappa_{2c}(t)$ found by Caroli *et al.* comes from the derivative term given in (3.10) which Maki neglected. Thus κ_{2M} is defined in terms of

$$f_1(\rho/2)=\sum_{n=0}^{\infty} n+\tfrac{1}{2}/(n+\tfrac{1}{2}+\tfrac{1}{2}\rho)^4,$$

i.e.,

$$(\kappa_{2M})^2=\frac{3}{2}\frac{f_1}{(\psi_2)^2}\frac{\lambda_L^2}{l^2}.$$

When the derivative term in (3.10) is applied to the Abrikosov form for $\Delta(\mathbf{r})$ its average just adds a factor of $\frac{1}{2}\rho$, resulting in a cancellation of one of the factors in the denominator. Therefore for κ_{2c}, which is the relevant parameter for *films in a perpendicular field* just as for bulk materials, f_1 is replaced by

$$-\tfrac{1}{2}\psi_3(\tfrac{1}{2}+\tfrac{1}{2}\rho)=\sum_{n=0}^{\infty}\frac{1}{(n+\tfrac{1}{2}+\tfrac{1}{2}\rho)^3},$$

i.e.,

$$(\kappa_{2c})^2=-\frac{3}{4}\frac{\psi_3}{(\psi_2)^2}\frac{\lambda_L^2}{l^2}.$$

For a *thin film in a parallel field*, derivatives of $\Delta(\mathbf{r})$ give contributions of order $\epsilon=[d/2\xi(t)]^2$ which may be neglected in the thin-film limit. Thus κ_{2M} should apply to this case.

For the case of *surface superconductivity* the Gaussian function is a good approximation and κ_{2c} applies just as in the Abrikosov state.

We expect a rather rapid change from κ_{2M} to κ_{2c} as the first vortices enter a film when $\frac{1}{2}d\sim\xi(t)$. To study in detail this behavior was a major aim of our work.

Let us look now at the left-hand-side integral L of (3.9). Just below H_M, the coefficient of $\Delta(\mathbf{r})$ (which is equal to zero at H_M) can be expanded to first order in the difference of the vector potential $\mathbf{A}$ from its value $\mathbf{A}_M$ at H_M,

$$L=\int dv(\mathbf{A}-\mathbf{A}_M)\frac{\delta}{\delta\mathbf{A}}\sum_{n=0}^{\infty}\frac{1}{(n+\frac{1}{2}+\frac{1}{2}\rho)}|\Delta(\mathbf{r})|^2. \quad (3.11)$$

Equation (3.9) may be used to form a free-energy functional of $\Delta(\mathbf{r})$ and $\mathbf{A}(\mathbf{r})$ by functional integration over Δ. As is well known from the GL approach, the minimization of the functional with respect to $\Delta^*(\mathbf{r})$ then gives back (3.9), while the minimization with respect to $\mathbf{A}(\mathbf{r})$ gives that the derivative of (3.11) is just the current $\mathbf{j}(\mathbf{r})$ [except for a factor $(1/4\pi\lambda_L^2)\times(6/V_F^2)$]. As obtained by Maki[6]:

$$\mathbf{j}(\mathbf{r})=\frac{1}{4\pi\lambda_L^2}\frac{3D}{2\pi T v_F^2}\psi_2(\tfrac{1}{2}+\tfrac{1}{2}\rho)\left\{\Delta^*(\mathbf{r})\left(\frac{\nabla}{i}-\mathbf{A}(\mathbf{r})\right)\Delta(\mathbf{r})+\Delta(r)\left(-\frac{\nabla}{i}-\mathbf{A}(\mathbf{r})\right)\Delta^*(\mathbf{r})\right\}, \quad (3.12)$$

with

$$\psi_2(z)=\psi'(z)=\sum_{n=0}^{\infty}\frac{1}{(n+z)^2}$$

and λ_L is the Landau penetration depth at $T=0$. From (3.11) we find

$$L=4\pi\lambda_L^2\frac{v_F^2}{6}\int dv(\mathbf{A}-\mathbf{A}_M)\cdot\mathbf{j}. \quad (3.13)$$

Gauge ambiguities may be removed by integrating by parts from a boundary b. One gets

$$L=4\pi\lambda_L^2(\tfrac{1}{6}v_F^2)\int dv(\mathbf{H}_M-\mathbf{H})\int_b \mathbf{dl}\times\mathbf{j}, \quad (3.14)$$

and finally

$$L=L_1+L_2=4\pi\lambda_L^2(\tfrac{1}{6}v_F^2)\int dv(\mathbf{H}_M-\mathbf{H}_A)\int_b \mathbf{dl}\times\mathbf{j}+4\pi\lambda_L^2(\tfrac{1}{6}v_F^2)\int dv 4\pi\left(\int_b \mathbf{dl}\times\mathbf{j}\right)^2. \quad (3.15)$$

The term L_1 occurs because the applied field H_A is less than H_M; it is proportional to $\langle|\Delta|^2\rangle$ ($\langle\ \rangle$ means an average over the volume). The term L_2 takes into account the effect of the screening currents in the film and is proportional to $\langle|\Delta|^4\rangle$. The same average appears in the expression for R which uses κ_2. We obtain a convenient expression for $|\Delta|^2$ by setting $L=R$,

$$|\Delta|^2=L_1|\Delta|^2/(R-L_2). \quad (3.16)$$

The magnetization $\mathbf{M}=\int dv\int_b \mathbf{dl}\times\mathbf{j}$ may be easily evaluated once $|\Delta|^2$ is known. The integrals L_1, L_2, and R have already been obtained and are discussed below for the three cases in which we are interested. Using the relations (3.2) and (3.4) the results can be written in a particularly convenient form:

(1) For a *thin film in a perpendicular field* the corrected results of Maki[6] give

$$S=\psi_2\frac{\rho}{H_M}\frac{(\kappa_{2c})^2}{\beta}\frac{1}{(\kappa_{2c})^2-\frac{1}{2}f(\eta)},$$

with

$$\beta=\frac{\langle|\Delta|^4\rangle}{(\langle|\Delta|^2\rangle)^2}=1.16,\quad \eta=\frac{d}{\lambda}, \quad (3.17)$$

$$(\kappa_{2c})^2=-\frac{3}{4}\frac{\psi_3}{(\psi_2)^2}\frac{\lambda_L^2}{l^2}.$$

We have used (3.8), which can be written

$$S=(\psi_3/8\pi^2T^2)|\Delta|^2/(H_M-H).$$

The last factor of expression (3.17) appears in all other quantities proportional to $|\Delta|^2$, such as the magnetization. The κ_{2c} in the numerator of (3.17) [and of later expressions (3.18) and (3.19)] is written only as a

convenient combination of polygamma functions in the calculation of S. A second-order transition is possible only when $(\kappa_{2c})^2$ is greater than $\frac{1}{2}f(\eta)$, since the square of the magnitude of Δ cannot be negative.

The function $f(\eta)$ calculated by Maki[32] takes into account the nonlocal electrodynamics and the field outside the sample which were not included in (3.15). When η is large these distortions are unimportant and $f=1$, but $f\to 0$ when $\eta\to 0$ (in particular when $T\to T_c$).

(2) For a *thin film in a parallel field* the results of Baratoff[10] give

$$S=\frac{\psi_2 2\rho(\kappa_{2c})^2}{H_M}\frac{1}{(\kappa_{2M})^2-\frac{1}{5}(d/\xi(t))^2}, \qquad (3.18)$$

with the Maki κ_2 in the denominator. A first-order transition must be obtained when the denominator is ≤ 0. Thus a second-order transition is possible when $d<\sqrt{5}\kappa_{2M}(t)\xi(t)$, which reduces to the GL result, $d<(\sqrt{5})\lambda(t)$, near T_c. The same requirement may be expressed in terms of H_{cB} using the forms for κ_1 and $\xi(t)$ given earlier,

$$\frac{H_M}{H_{cB}}>\left(\frac{24}{5}\right)^{1/2}\frac{\kappa_1(t)}{\kappa_2(t)}.$$

(3) For *thick film in a parallel field* Maki[33] has evaluated the integrals using the approximation of a Gaussian wave function. Substituting the correct κ_2 function, we obtain

$$S=\frac{\psi_2\sqrt{2}\rho(\kappa_{2c})^2}{H_M}\frac{1}{\kappa_{2c}^2-0.156}. \qquad (3.19)$$

The denominator requires a first-order transition for $\kappa_{2c}<0.56/\sqrt{2}$ or $H_{c3}/H_{cB}<0.95\kappa_1/\kappa_{2c}$, but $H_{c3}<H_{cB}$ is a stronger requirement.

The particular advantage of presenting the theoretical formulas for S in this form, in addition to emphasizing their similarity, is that only one experimental number H_M is necessary to fix the scale for the formula.

The field H_M can be measured accurately for several temperatures and the best fit to the function $1/\tau(t)$ found. After the scale is thus fixed at any one temperature, universal functions of t give the complete temperature dependence. Most commonly these formulas have been presented[11b] in a form which requires knowledge of σ and κ to fix the scale. As we discussed in Sec. II, we cannot determine these parameters to better than 10% accuracy. With such uncertainties in the scale, combined with experimental errors in S, a good determination of the temperature dependence of κ_2 would be more difficult. Also, in this new form many of the corrections due to the finite value of l cancel out. These corrections are considered further in Appendix I and in the following sections, where we compare the theory with experiment.

IV. THIN FILMS IN A PERPENDICULAR MAGNETIC FIELD

We first present our results for the case of a thin film in a perpendicular field. The only differences between this case and a bulk type-II superconductor penetrated by vortex lines as given by Abrikosov are: (a) the effects due to the field outside the specimen[34]; (b) the effects due to the scattering of electrons at the boundary.

The temperature dependences of the critical field and $|\Delta|^2$ have been studied previously by one of us[11b] on the same **In**Bi alloys used here and one finds that (a) the fit with theory was good for the critical field, and (b) a deviation from theoretical values for $|\Delta|^2$ was presented in terms of a κ_2 parameter increasing more than κ_{2c} when T decreased. Since there are actually several corrections that occur when $l/\xi_0\neq 0$, which may or may not be included in the parameter κ_2, we prefer to compare theory directly with the measured quantity $D(V)$. The results obtained agree with the earlier ones for thick samples[11] but are now presented in the following sections. The results are discussed in the light of the recent paper by Maki[32] on the fluxoid structure in perpendicular geometry.

A. Critical Fields

Values of $H_M(t)=H_\perp(t)$ are shown in Fig. 2. They agree with the theoretical prediction given by Eqs. (3.2), (3.3), and (3.4). The effective mean free path of the thinnest films l_{eff} is reduced by boundary scattering. This causes an increase of $H_\perp$. From $H_\perp$ we can deduce $\xi(t)$ using the relation $\xi(t)^2=1/H_\perp$. A typical set of data for an **In**Bi 2.5% alloy gives $T_c=4.1$°K and

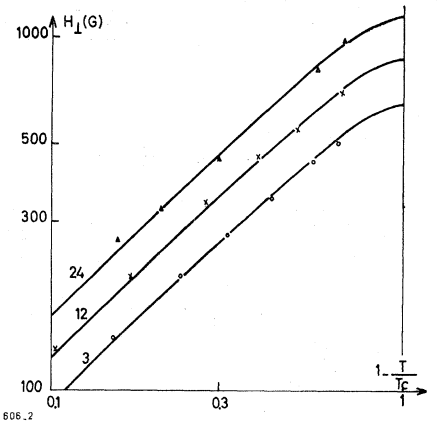

FIG. 2. Variation of the prependicular critical field with temperatures. The slope 1 near T_c says that $H\propto(T_c-T)$. The best fit with the theoretical (continuous) curve obtained by its translation along the H axis gives the κ of the film. The thickness of the films decreases from 3 to 24.

[32] K. Maki, Ann. Phys. (N. Y.) **34**, 363 (1965).
[33] K. Maki (unpublished).
[34] J. Pearl, Appl. Phys. Letters **5**, 65 (1964).

$\xi(t)=700(1-t)^{-1/2}$ Å (for $t>0.7$). The residual resistivity $\rho_R=3.5\times10^{-6}$ Ω cm together with the dirty-limit form[27b] $\xi(t)=0.85(\xi_0 l)^{1/2}(1-t)^{-1/2}$ gives us the value of the product $\rho_R l\xi_0=1.6\times10^{-16}$ Ω cm^3 before corrections of order l/ξ_0 are considered. [Boundary-scattering corrections cancel in this product because they are the same for $\xi(t)^2$ and $\sigma_R=1/\rho_R$. We have found by averaging over samples of different thicknesses (and concentration) $\rho_R l\xi_0=1.55\pm0.10$.] This value of $\rho_R l\xi_0$ is already roughly compatible with the values proposed by one of us[29] by fitting his theory for the parallel critical fields of thin films to Toxen's experiments[17] ($\xi_0=2700$ Å, $\rho_R l=1.1\times10^{-11}$ Ω cm^2), but not with the data proposed by Toxen ($\xi_0=2600$ Å, $\rho_R l=2.0\times10^{-11}$ Ω cm^2) from his own model. The product is also compatible with the values suggested by Dheer[15] ($\xi_0=4400$ Å, $\rho_R l=0.57\times10^{-11}$ Ω cm^2). However, this last value of ξ_0 was seen to be too large to fit the experimental data of Toxen.[24] The value of $\rho_R l$ is also too small with respect to other results (see also Sec. II G). We use a value $\rho_R l=1.0\times10^{-11}$ Ω cm^2, which gives $l=290$ Å for the 2.5% **In**Bi described, to calculate the corrections of order l/ξ_0 to the value $\rho_R l\xi_0=1.6\times10^{-11}$ Ω cm^2. According to the Gor'kov theory[3] the expression for $\xi(t)$ is corrected as follows:

$$\xi^2(t)(1-t)=(0.851)^2\xi_0 l\times\left[1+\frac{8}{\pi^2}\frac{1}{2\rho_G}\left\{\psi(\tfrac{1}{2})-\psi\left(\frac{1}{2}+\frac{\rho_G}{2}\right)\right\}\right], \quad (4.1)$$

where $\rho_G=0.882\ \xi_0/l$. The digamma function may be expanded[35] in a power series in ρ_G^{-1}, giving finally

$$\xi^2(t)(1-t)=(0.851)^2\xi_0 l\left[1-\frac{l}{\xi_0}\left\{0.527-0.460\ln\frac{l}{\xi_0}\right\}-0.0984\left(\frac{l}{\xi_0}\right)^3+\cdots\right]. \quad (4.2)$$

A self-consistent calculation for ρ_0 using this last formula and the value of l gives a corrected expression for $\rho_R l\xi_0$: $\rho_R l\xi_0=1.6\times10^{-16}(1-0.203)^{-1}$ Ω cm$^3=2\times10^{-16}$ Ω cm^3 and $\xi_0=2000$ Å ($l/\xi_0=1/7$). If we assume that v_F is not modified when impurities are added to In, the value of ξ_0 for pure In deduced from the T_c (4.1°K for the alloy, 3.41°K for pure In) is $\xi_0=2400$ Å, which is in satisfactory agreement with the earlier suggestion, 2700 Å,[29] and that of Toxen, 2600 Å.[18]

Corrections: As we remarked at the end of Sec. III, the theoretical formulas for S have been written so that we need not know the precise values of the corrections. We include them in an effective value of l, called l_{eff}. The corresponding value of κ_{eff} deduced from the values of the perpendicular critical field applies to the formula for S in the perpendicular geometry. The same κ_{eff} does not apply to the same film in a parallel field, however, since the corrections are different. For the three films shown in Fig. 2, for sample, $\kappa_{\text{eff}}=0.98$, 1.36, and 1.63 may be corrected using Fuch's theory[28] and the value of d deduced from the $H_{||}$ to give $\kappa=0.88$, 1.13, and 1.18 for films Nos. 3, 12, and 24, respectively. The largest correction factor, 0.72, is obtained for the thinnest film, No. 24, where l nearly equals d. (The increase in the values of κ is due to a small increase in Bi concentration.)

B. Amplitude Effects

Figure 3 shows $D_{V=0}(H)$ for a film of intermediate thickness ($d=1900$ Å). In a perpendicular field $D(H)$ is nearly a linear function of H from O to H_M. The value of the first-entry field is too small to be observed, because of the large demagnetizing factor, which precludes any flux exclusion. This linear general behavior is expected from the GL theory, since the eigenvalue $1/\tau_K$ is linear in H (3.4):

$$\frac{1-D(H)}{1-D(O)}=\frac{|\Delta(H)|^2}{|\Delta(O)|^2}=1-\frac{H}{H_M}.$$

Experimental results for the slope S (2.2) are presented in Fig. 4 together with theoretical curves. The main qualitative feature is the relative constancy of S for different thicknesses and temperatures, which contrasts sharply with the following results for parallel fields (Secs. V and VI B).

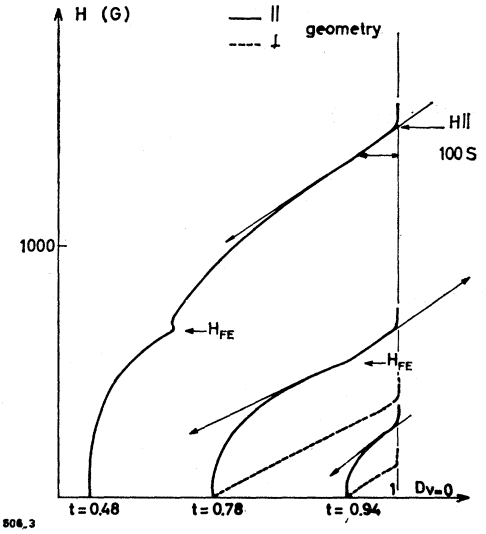

FIG. 3. Variation of the normalized initial slope of the tunneling characteristics with field. The high-field part of the $t(=T/T_c)=0.48$ curve shows typical determinations of the slope S on a 100-G interval and of the upper critical field (H_{11}). The parallel-field curve at $t=0.9$ does not show the break which we associate at lower temperatures with the first entry of vortices in the film (H_{FE}). The structure at the break is usually more pronounced when $H_{FE}<H_{c2}$ (curve $t=0.48$). The perpendicular-field curves are nearly linear over the whole temperature range.

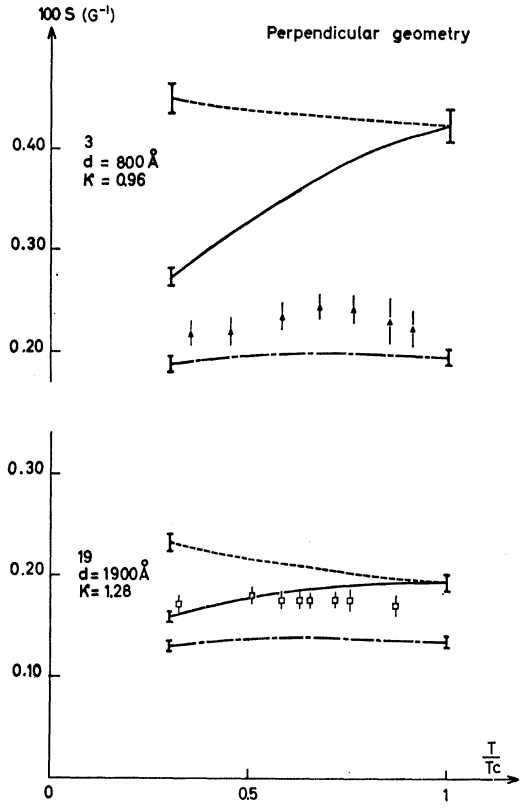

FIG. 4. Temperature dependence of S in perpendicular geometry. The theoretical curves were calculated using values of κ determined from H_1; dashed line: dirty limit form with $f=1$; solid line: corrected curve with $f=1$ using the finite value of l/ξ_0; dashed and dotted line: corresponding corrected curve with $f=0$. Our experimental results on thick (No. 19) and thin (No. 3) samples indicate that the effect of screening currents becomes smaller near T_c and for thinner films: $f\to 0$ when $d/\lambda(T)\to 0$.

Equation (3.17) gives the theoretical curve in the dirty limit ($l\ll\xi_0$) when $f(\eta)=1(\lambda\ll d)$:

$$S=\psi_2\rho(\kappa_{2c})^2/\beta H_M 1/((\kappa_{2c})^2-\tfrac{1}{2}). \qquad (3.17')$$

The relative constance of S follows from the linearity of the GL eigenvalue of H_M, $\rho=DH_M/2\pi T$. The temperature variation of H_M and ρ, each as $1-t$ near T_c, cancel.

Although the corrections arising from the finite ratio l/ξ_0 do not change the temperature dependence of κ_1, they have a large effect on κ_2. Our earlier experiments indicated a κ_2 parameter which increased roughly twice as fast as κ_{2c} as the temperature was lowered. On the other hand, our calculations in Appendix I for the corrections to the appropriate parameter for a thin film κ_{2M} indicate a correction which results in a corrected parameter $\kappa_{2M}{}^*=\kappa$ independent of t for the particular value $l/\xi_0=\frac{1}{9}$ (see Sec. V B). To reconcile the theory with these earlier and our present experiments we *assume* that a correction of the same magnitude applies to all the κ_2 parameters for this ratio of l/ξ_0. Hence we replace κ_{2c} in the denominator of (3.17') by a corrected value $\kappa_{2c}{}^*=\kappa_{2c}(\kappa/\kappa_{2M})$ to obtain our corrected theoretical curve with $f(\eta)$ still equal to 1.

$$S=\psi_2\frac{\rho(\kappa_{2c})^2}{H_M\beta}\frac{1}{(\kappa_{2c}{}^*)^2-\frac{1}{2}}. \qquad (3.17'')$$

This correction is seen in Fig. 4 to bring the theory closer to experiment.

At this point one could in principle deduce the values of Maki's function $f(\eta)$ from the experimental values by replacing the $\frac{1}{2}$ in the denominator of Eq. (3.17'') by $\frac{1}{2}f(\eta)$. However, the experimental situation is not favorable for an accurate determination of $f(\eta)$. In order to obtain reasonably dirty films our values of κ must be larger than 1, and our errors in the determination of S and $\kappa_{2c}{}^*$ would give rise to large errors in the value of $f(\eta)$ deduced from them. We prefer to show the limiting curve for $f(\eta)=0$,

$$S=\psi_2\frac{\rho\kappa_{2c}{}^2}{H_M\beta}\frac{1}{\kappa^*{}_{2c}{}^2}=\psi_2\frac{\rho}{H_M\beta}\left(\frac{\kappa_{2M}}{\kappa}\right)^2, \qquad (3.17''')$$

and compare the experimental data with the theoretical limits (3.17'), (3.17''), and (3.17''').

We give such a comparison in Fig. 4 for a thin (No. 3) and a thick (No. 19) film:

$$\text{No. 3, } d=800\text{ Å}, \quad \eta=\frac{d}{\kappa\xi(t)}=\frac{800}{(1.0)(590)}(1-t)^{1/2};$$

$$\eta>1 \quad \text{for} \quad t>0.45,$$

$$\text{No. 19, } d=1900\text{ Å}, \quad \eta=\frac{1900}{(1.3)(510)}(1-t)^{1/2};$$

$$\eta>1 \quad \text{for} \quad t>0.88.$$

The experimental results show the expected results: (a) Those of No. 3 do not deviate much from the corrected $f=0$ curve; (b) those of No. 19 follow the corrected $f=1$ curve at low temperature and go towards the $f=0$ one at higher temperature.

V. THIN FILMS IN A PARALLEL FIELD

Next we consider the films whose thickness is much smaller than the diameter of a vortex ($\sim 2\xi(t)$) when a magnetic field is applied parallel to the surface. Since $\xi(t)$ is the characteristic distance over which the pair potential varies, $|\Delta|$ may be considered constant for these thin films.

A. Critical Field

According to Eqs. (3.4) and (3.5) the temperature dependence of $H_{\parallel}{}^2$ should be the same as $H_\perp$ in the dirty limit. In particular, near T_c, $H_{\parallel}$ is proportional to $(1-t)^{1/2}$, whereas $H_\perp\propto(1-t)$. This point was used to determine T_c by extrapolating to zero the linear part of the $H_{\parallel}{}^2(T)$ curve. The agreement of our experiments with the dirty-limit theory, shown on Fig. 5, is very

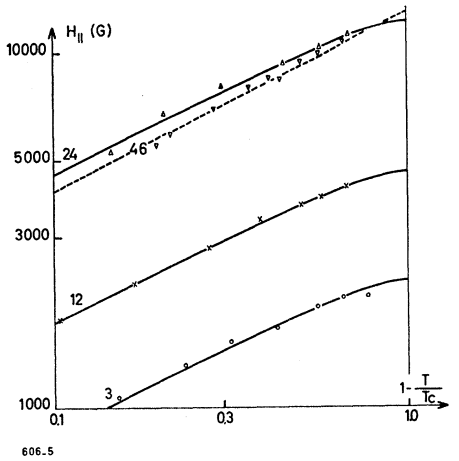

FIG. 5. Temperature variation of the parallel critical fields of thin films [$d<\xi(t)$]. For the alloy films (Nos. 3, 12, 24) we find a good agreement with the theoretical (solid line) variation: $H_{II}\propto H_{\perp}^2$. The variation of $H_{II}(T)$ is more pronounced at low T for the pure thin In film (No. 46), as is seen from comparison with the line $(1-t)^{1/2}$ (dashed line). The calculated thicknesses are: No. 3, $d=800$ Å; No. 12, $d=470$ Å; No. 24, $d=230$ Å; No. 46, $d=300$ Å.

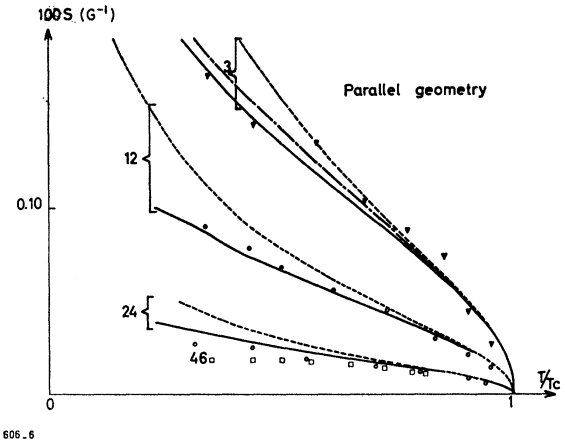

FIG. 6. Temperature variation of the slope in parallel geometry for the same thin films as in Fig. 5. The amplitude of the theoretical curve, which keeps a universal form, is solely determined from the data of H_{II}. Dashed line is for the dirty-limit formula (3.18′); solid line is for the corrected formula (3.18″). The curve (dashed and dotted line) for the thicker film (No. 3) take into account the correction due to thickness. The variation for the pure In film (No. 46) is to be compared to that of the alloy film (No. 24) of comparable thickness.

good: $\kappa_1(t)$ follows the Maki form[6] and does not depend strongly on the requirement $l/\xi_0\to 0$.

We have deduced the values of the thickness from the critical fields using

$$d^2=12H_{\perp}f_F/H_{II}^2f_D,$$

where $f_F(l/d)$ is the correction due to boundary scattering for perpendicular fields as calculated from Fuch's theory:[23] $l_{\text{eff}}=lf_F$, and $f_D(l/d)$ is the correction, due to both boundary scattering and nonlocality, for parallel fields, which we calculated earlier.[29] The values of d deduced in this way are consistent with our optical and resistive determinations.

We have also made thin films of pure In to look for the much more rapid increase in $H_{||}$ at low temperature predicted by de Gennes and Tinkham[12] and by Shapoval.[36] However we have only found small corrections of the same order ($\sim 10\%$) as those we explained for a moderately dirty film.[29] The resulting behavior is seen from Fig. 5 to be a 5% deviation below $(1-t)^{1/2}$ behavior, contrasting with the 5% deviation below $(1-t)^{1/2}$ given by Maki's theory for the dirty films. However, we note that strains[17] have increased the T_c of this pure film to 3.73°K [T_c(Bulk In)=3.41°K], so that we cannot be sure that l is larger than ξ_0 for these thin films.

B. Amplitude Effects

A typical curve of $D_{V=0}(H)$ for a thin film is given in Fig. 3 ($t=0.94$). The shape of $D(H)$ is roughly what would be expected from the GL theory:

$$\frac{1-D_{V=0}(H)}{1-D_{V=0}(O)}=\frac{|\Delta(H)|^2}{|\Delta(O)|^2}\sim 1-\left(\frac{H}{H_M}\right)^2.$$

In a domain of field typically $0.7H_M$ to H_M, the function $D_{V=0}(H)$ varies linearly, and no sudden anomalies are seen on the curves.

In Fig. 6 we present experimental determinations of the slope S in the high field region. The qualitative features of the curves are the increase in S with thickness and the $(1-t)^{1/2}$ behavior near T_c as expected from (3.5).

As discussed in Sec. IV B, κ_2 (in contrast to κ_1) does show important corrections from the temperature variation in the dirty limit for our **In**Bi alloys. We show in Appendix I that the appropriate parameter for a thin film, κ_{2M}, should be corrected to be approximately independent of temperature for $l/\xi_0\sim\frac{1}{9}$, its value being

$$\kappa_{2M}{}^*=\kappa=\kappa_{2M}(\kappa/\kappa_{2M}).$$

κ_1 keeps the dirty-limit form.

All corrections studied in Appendix I may be incorporated in κ_{2M} (see discussion of the results of Table II). The $(\kappa_{2c})^2$, which we placed in the numerator of (3.18) as a convenient combination of polygamma functions, remains unchanged.

The theoretical curves shown in Fig. 6 are obtained from Eqs. (3.18), below. When $\kappa\geq 1$ we neglect the term $\frac{4}{5}\epsilon$ in the denominator ($\epsilon\ll 1$ in the thin-film regime). Therefore the theoretical formula valid in the dirty limit is

$$S=\psi_2\frac{2\rho\kappa_{2c}{}^2}{H_M}\frac{1}{\kappa_{2M}{}^2}. \qquad (3.18')$$

[35] Janhke, Emde and Losch, *Tables of Higher Function* (McGraw-Hill Book Publishing Company, New York, 1960). Note that their definition of the origin of the digamma function is different from the one used here by -1.

[36] E. A. Shapoval, Zh. Eksperim. i Teor. Fiz. **49**, 930 (1965) [English transl.: Soviet Phys.—JETP **22**, 647 (1966)].

The corrections due to the finite ratio $l/\xi_0(\sim\frac{1}{9})$ give the corrected formula

$$S=\psi_2\frac{2\rho\kappa_{2c}^2}{H_M}\frac{1}{\kappa^2}. \qquad (3.18'')$$

These curves have a universal temperature dependence independent of κ. The scale factor is completely given by the value of H_M.

For the thickest film (No. 3) shown in Fig. 6, at the lowest temperature, $\epsilon\sim\frac{1}{4}$ is not negligible. We have calculated the curve taking into account the finite value of ϵ.[37]

The experimental results for a pure In film (No. 46) are shown on Fig. 6. If we used a dirty-limit approach, the curve for film No. 46 should be higher than that of film No. 24 because H_M is slightly smaller (see Fig. 5). We see the opposite and reasonable result in Fig. 6: The deviation of the slope of pure In film from the dirty limit goes in the same sense as for the alloy films and is more pronounced.

If in (3.18′) κ_{2M} were replaced by κ_{2c}, which is the appropriate parameter for bulk type-II superconductors, the theoretical curves would be divided by 1.7 at $t=0.3$. Such a deviation is outside the range of experimental error. Thus we may definitely conclude that the κ_2 parameter for our not-too-dirty films is nearly constant. The ratio of this κ_2 to that determined on the same films in perpendicular geometry is smaller than 1 and is still given by $\sim\kappa_{2M}/\kappa_{2c}$, as assumed in Sec. IV B.

VI. FILMS OF INTERMEDIATE THICKNESS IN PARALLEL FIELDS

When the thickness of a film exceeds the diameter of a vortex $[\sim 2\xi(t)]$ new phenomena occur which we associated with the entry of flux lines into the film. Typical tunneling measurements are shown in Fig. 3 for a film $d=1900$ Å. Near $T_c[(d/\xi(t))<1]$, we observe thin-film behavior. When the temperature is lowered, a simple discontinuity of slope occurs, first at H_M and then below H_M at lower temperatures. This simple break is shown for the curve $t=0.48$ and defines a field H_{FE}. There is little irreversibility in the curve near H_{FE} and we expect it to define a thermodynamic field value. The break first appears at a point defined by $H_{FE}=H_M$, which was identified for numerous samples by the constant ratio

$$\frac{H_{II}}{H_\perp}=1.98\pm0.05 \quad \text{or} \quad \epsilon=\epsilon_{cr}=0.816.$$

The same ratio was found to correspond to the sharp maximum of the angular dependence curves[24] near H_{II}; it was associated with the change in the solution of the linearized GL equation from a one-dimensional and symmetric one to a two-dimensional solution peaked near a boundary (or equivalently to the creation of vortices in the film).

At lower temperatures ($t=0.48$ of Fig. 3) the flux lines enter the film when H is far from H_M and the change in the tunneling characteristics is more complicated. Such complicated anomalies for thick films have been recently observed by Sutton[38] and have also been interpreted in terms of flux entry. However, he did not report the case which primarily interests us here, when the flux entry occurs in the high-field region.

A. Critical Fields

The variation of H_{II} with d and T has been studied extensively before.[26] The results are conveniently presented on the universal $\epsilon(h)$ curve[5] as shown in Fig. 7. In addition we present values for the first-entry field H_{FE} which is seen also to define a unique curve near ϵ_{cr}. The field H_{FE} becomes smaller than H_{c2} without any break, although complicated transitions are seen when $H_{FE}<H_{c2}$.

For very thick films H_{FE} is limited by $H_{FE}>H_{c_1}$. (For a 8000 Å InBi 2.5% alloy we find $H_{FE}=180\pm10$ G at 2.55°K, whereas Kinsel[21] gives $H_{c_1}=175$ G). For these films the results for $H_{FE}\sim H_{c_1}$ (not shown on Fig. 7) are spread as a function of ϵ because H_{FE} becomes in fact a function of d/λ as shown by Abrikosov.[39] A presentation of this field would require a three-dimensional diagram with a new variable d/λ.

The fact that we observe very little irreversibility, whereas barriers for flux entry have been predicted for thick films,[40] is probably related to the unfavorable

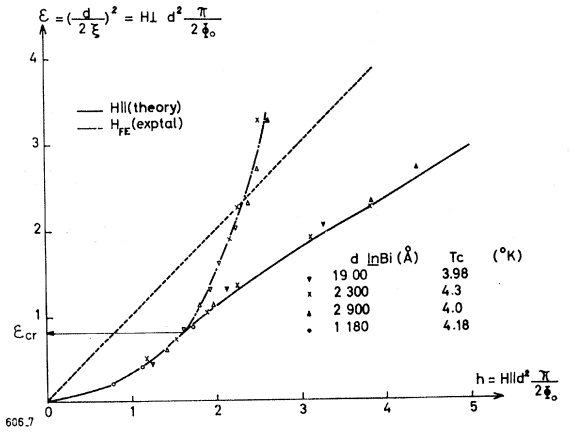

FIG. 7. General diagram for $H_\perp$, H_{II} and for the first-entry field H_{FE}. The theoretical curve is that of Ref. 5. For $\epsilon<\epsilon_{cr}$ one gets nearly the GL-limit result $\epsilon=\frac{1}{3}h^2$ and no H_{FE} is seen. For $\epsilon>\epsilon_{cr}$ there is an H_{FE} and one goes rapidly to the thick-film limit $h/\epsilon=1.69$. No anomaly is seen around the point $H_{FE}=H_{c2}$.

[37] This correction can be calculated easily by constructing a perturbation theory in powers of $d/\xi(t)$. We do not present the results of such a calculation because the numerical results given in the next section are more general, being valid for all thicknesses.

[38] J. Sutton, Proc. Phys. Soc. (London) **87**, 791 (1966).

[39] A. A. Abrikosov, Zh. Eksperim. i Teor. Fiz. **46**, 1464 (1964) [English transl.: Soviet Phys.—JETP **19**, 988 (1964)].

[40] P. G. De Gennes, Solid State Commun. **3**, 127 (1965).

presence of the edges of our flat films. Calculations and further experimental study of H_{FE} as well as hysteresis effects are in progress in Orsay.

B. Amplitude Effects

Figure 8 gives the slope S for a film which shows the same features as that of Fig. 3. Near T_c, the slope S has the parabolic behavior characteristic of a thin film. The break at $H_{FE}=H_{II}$ is clearly displayed and corresponds to a theoretical discontinuity of 3/2. We have also shown the values of the slope before the flux enters, when $H_{FE}<H_{II}$, corresponding to the unstable one-dimensional solutions. At low temperature S has the characteristics of a thick film with surface superconductivity: They are very similar to those for the bulk type-II vortex structure discussed in IV.

The theoretical curves have been obtained by a numerical integration presented in Appendix II. The corrected curves used the assumed universal corrections for our alloys $(l/\xi_0\sim\frac{1}{9})$, $\kappa_2\rightarrow\kappa_2{}^*=\kappa_2(\kappa/\kappa_{2M})$.

Let us discuss first the vortex state:

The solution[41] $\Delta(x,y)=e^{iky}F(x)$ of the linearized GL equation which satisfies the boundary condition[7] $(d\Delta/dx)_{x=\pm d/2}=0$ has been computed by Saint James for all values of ϵ. He found $k=0$ and F symmetric about the center and practically constant for $\epsilon<0.816$. For $\epsilon>0.816$, k increases very rapidly and F becomes asymmetric, having larger values near one boundary than near the other. The solution $e^{-iky}F(-x)$ obtained by a reflection through the origin is equally valid. The appropriate solution[26,42] for one row of vortices is just a linear combination of the two solutions with arbitrary phase factors which may be chosen for convenience.

$$\Delta(x,y)=e^{iky}F(x)+ie^{-iky}F(-x). \tag{6.1}$$

The magnitude of $|\Delta|^2$ is symmetric about the film center:

$$|\Delta|^2=F^2(x)+F^2(-x)+2F(x)F(-x)(\sin 2ky). \tag{6.2}$$

The vortices are centered at the points $x=0$, $2ky=-\frac{1}{2}\pi+2n\pi$ (n integer) since $|\Delta|^2=0$ there. The currents are given, using (3.12), by

$$\begin{aligned} j_y&=-K\{H_x(F^2(x)+F^2(-x)+2F(x)F(-x)\sin ky)\\ &\qquad -k(F^2(x)-F^2(-x))\}, \\ j_x&=-K\{F'(x)F(-x)-F(x)F'(x)\}\cos 2ky, \end{aligned} \tag{6.3}$$

where

$$K=\frac{1}{4\pi\lambda_L{}^2}\frac{3D}{\pi T v_F{}^2}\psi_2\left(\frac{1+\rho}{2}\right).$$

Thus in addition to the currents flowing parallel to the film boundaries independently of y, there are vortices of current circling the points where $|\Delta|^2=0$.

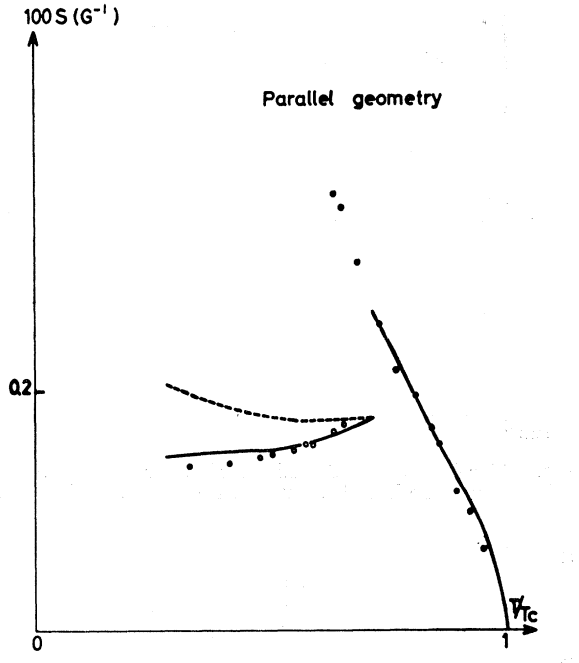

FIG. 8. Temperature variation of the high-parallel-field slope for an intermediate-thickness film showing the same behavior as in Fig. 3. The jump in slope is associated with the first occurence of flux entry. The theoretical curve was fitted at the maximum value $S=0.26$ and gives the right magnitude of the jump. At lower temperature, S is nearly constant, as in the perpendicular geometry case. Dashed line is the corresponding calculated curve in the dirty limit.

The discontinuity in the slope S comes entirely from a discontinuity in $\langle|\Delta|^4\rangle$ (average over the volume of the film) or more precisely in the parameter $\beta=\langle|\Delta|^4\rangle/(\langle|\Delta|^2\rangle)^2$ which appears in the denominator of expression (3.16) for $|\Delta|^2$. The magnitude of the discontinuity may be easily obtained by approximating F by a constant, which remains a good approximation just above $\epsilon=0.816$. For $\epsilon<0.816$, $k=0$ and $\beta=1$. For $\epsilon>0.816$, k becomes finite. The magnitude of $\langle|\Delta|^2\rangle$ does not change, since the average of the sine in (6.2) is zero. The term $4(\sin^2 2ky)F^2(x)F^2(-x)$ of $|\Delta|^4$, which averages to zero for $k=0$, gives $2F^2(x)F^2(-x)$ as soon as $k\neq 0$. Hence β changes discontinuously to $\frac{3}{2}$.

From the relation (3.16) one sees that the slope S, proportional to $|\Delta|^2$, becomes less by $\frac{2}{3}$. The observation of a change of slope of this value is a rather striking confirmation of the vortex nature of the solution for $\epsilon>0.816$.

Using the expressions (6.1) and (6.3) for Δ and $\mathbf{j}$, we write explicitly in Appendix II the integrals L_1, L_2, and R ($B1$, 2, 3) which must be evaluated numerically. In the dirty limit, S is written in terms of the three functions, J_1, J_2, and C, which are displayed in Figs. 9, 10,

[41] The origin $y=0$ is arbitrary for the infinite system considered here. H is along the z axis.

[42] A complete treatment is given in *Type* II *Superconductivity*, by D. Saint James, G. Sarma, and E. J. Thomas (Pergamon Press, Inc., to be published).

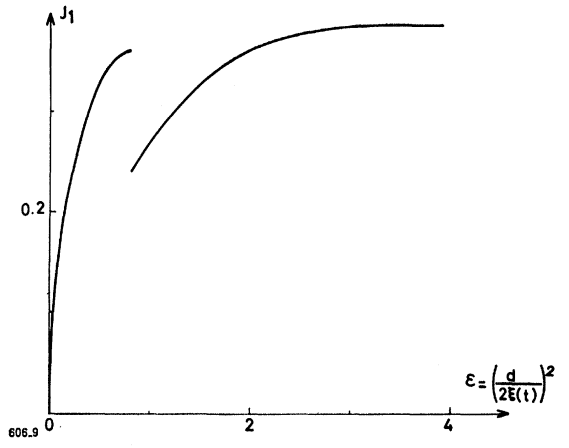

FIG. 9. The functions J_1, J_2 and C are used to calculate S for all thicknesses. The jump in J_1 at ϵ_{cr} is responsible for that of S.

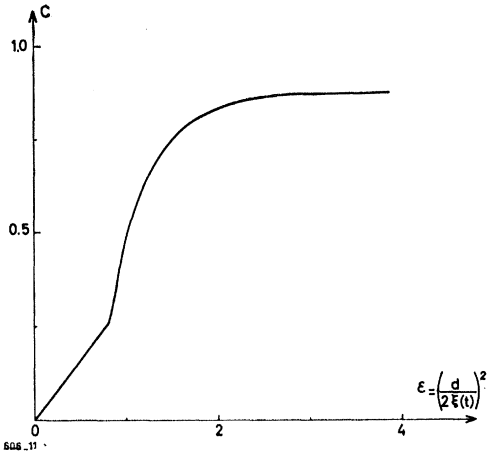

FIG. 11. C shows the variation of the parameter κ_2 from the Maki limit ($C=0$) to that of Caroli *et al.* ($C=1$).

and 11.

$$S=\frac{(\kappa_{2c})^2(D/\pi T)\psi_2 J_1}{(\kappa_2)^2-J_2}, \tag{6.4}$$

with

$$(\kappa_2)^2=(\kappa_{2M})^2(1-C)+C(\kappa_{2c})^2. \tag{6.4'}$$

Each of the three functions has a discontinuity of slope at ϵ_{cr}. J_1 has an additional discontinuity of $\frac{3}{2}$, since we have included the factor β^{-1} in its definition. J_1 is an integral of the current and J_2 is the square of an integral of the current. These integrals indicate the decrease in the field strength inside the superconductor caused by the screening currents.

The quantity J_2 is a measure of the effectiveness of these currents in screening the magnetic field. In particular, a first-order transition must occur when J_2 exceeds $(\kappa_2)^2$, as the magnitude of $|\Delta|^2$ cannot be negative. We will discuss this point in Sec. VII.

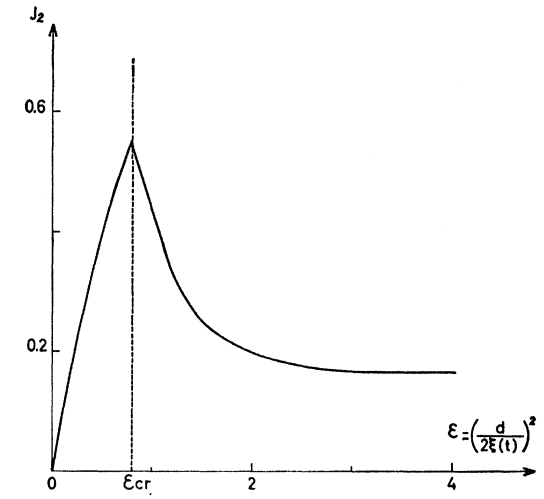

FIG. 10. J_2 shows the strength of screening currents. It goes to zero with ϵ; screening currents become negligible for thin films. It also decreases when the two sheaths of the surface state become farther apart. It is at a maximum with almost the value for the Abrikosov bulk type-II case at the point where the film can just accommodate vortices at H_M.

The parameter C defined in (4.4') measures the strength of the derivatives of $|\Delta|^2$. In the thin-film limit, C goes to 0 and $\kappa_2 \to \kappa_{2M}$. In the thick-film limit, as in the bulk type-II case, C goes to 1 and $\kappa_2 \to \kappa_{2c}$.

Table I gives the values of all three functions in some particular cases.

The value of D in (4.4) is easily obtained by fitting the accurately determined value of H_M at the break on the curve $\epsilon(h)$ at the point $\epsilon=\epsilon_{cr}$.

According to our assumed universal correction for our alloys ($l/\xi_0 \sim \frac{1}{9}$), the corrected value of κ_2 is obtained from (4.4') by multiplying by κ/κ_{2M}:

$$(\kappa_2^*)^2=\kappa^2[(1-C)+C(\kappa_{2c}/\kappa_{2M})^2]. \tag{4.5}$$

Only near ϵ_{cr}, where J_2 is at a maximum, is the theoretically obtained value of S somewhat sensitive to the chosen value of κ. In order to fit the experimental value of the maximum in Fig. 8 we were led to choose $\kappa=1.13$ for the uncorrected formula and $\kappa=1.05$ for the corrected one. A value of $\kappa=1.20$ is deduced from $H_\perp$ measurements, but as discussed in Sec. IV A, such discrepancies are not unexpected.

TABLE I. Behavior of functions J_1, J_2, C, of the expression of the slope in high field [Eq. (6.4)].

	$\epsilon \to 0$	$\epsilon_{cr}=0.816$	$\epsilon=3.8$	$\epsilon \to \infty$ (Gaussian approx.)
J_1	$\frac{Hd^2}{12}=\left(\frac{\epsilon}{3}\right)^{1/2}$	0.361; 0.241	0.387	0.418
J_2	$0.80\,\epsilon$	0.539	0.165	0.156
C	$0.30\,\epsilon$	0.259	0.878	1.00

The low-temperature results are insensitive to the magnitude of κ chosen and show that the temperature dependence of $\kappa_2(t)$ has become that for samples in perpendicular fields, which increases approximately as $\kappa\kappa_{2c}/\kappa_{2M}$.

Figure 12 shows the theoretical dependence for $\kappa_2(t)$ calculated in the dirty limit for a film having the same $\epsilon(t)$ as our film. This is the uncorrected form used to calculate the upper curve of Fig. 8. Figure 13 shows the corresponding function κ_2^*, which gives good agreement with our experiments. The corrected and uncorrected forms of κ_{2c} applying to bulk type-II case are shown for comparison. The corrected κ_{2M} for a thin film is just the horizontal axis in this last figure.

VII. NUCLEATION DIAGRAM FOR PARALLEL FIELDS

A particularly interesting feature of Fig. 10, showing the function $J_2(\epsilon)$, is that it gives the type of transition to the normal state. If we add the vertical line $\epsilon=\epsilon_{cr}$, this diagram also gives the character of the solution for Δ near the nucleation field. We show Fig. 10 redrawn with the horizontal axis replaced by d/λ in Fig. 14. We do not distinguish κ_1 from κ_2 for the present qualitative description of this diagram, but assume them equal to a constant κ, as is strictly true only near T_c. The function J_2 defines the boundaries of a region I in which a first-order transition must occur at H_M. In region I, $\kappa^2<J_2$, and small values of $|\Delta|^2$ are not possible, since they cannot be negative [see (IV.4) and note that $S\propto|\Delta|^2$]. The requirement $\kappa^2<J_2$ reduces to the well-known requirement $d>(\sqrt{5})\lambda$ in the thin-film region ($\epsilon\to 0$),[43] and to $\kappa<0.59/\sqrt{2}$ in the thick-film region ($\epsilon\to\infty$), so that in the latter case $H_{c3}<H_c$. In the rest of the diagram (II) a second-order transition to the normal state is possible. To the left of the dotted curve ($\epsilon=\epsilon_{cr}$) the solution for Δ is one-dimensional (region S) with no distinction between surface and bulk behavior. To the right Δ contains vortices at H_M and has a two-dimensional character—state II σ. The same distinction with respect to the curve $\epsilon=\epsilon_{cr}$ applies to the supercooling fields in region I.

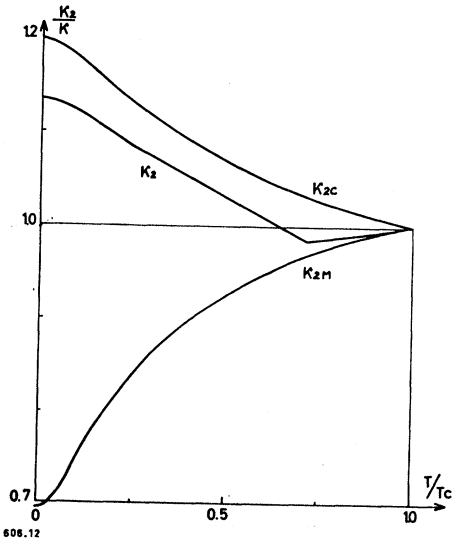

FIG. 12. The limiting form for κ_{2M} and κ_{2c} and that for the film of Fig. 8 as a function of T/T_c in the dirty limit.

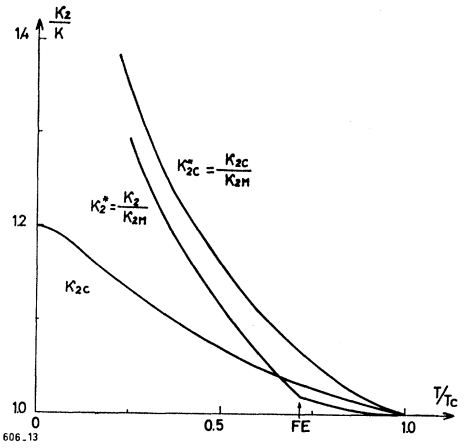

FIG. 13. The corrected forms corresponding to Fig. 12 for a finite value of $l/\xi_0\sim 1/g$.

In thick films we may easily distinguish between bulk and surface behavior and separate the diagram of Fig. 14 further in two regions: If $\kappa>1/\sqrt{2}$, the Abrikosov mixed state is possible in the bulk, and there will be a second-order transition in the bulk (2) at H_{c2} [i.e. (2) II σ]. If[44] $0.59/\sqrt{2}<\kappa<1/\sqrt{2}$, there will be a first-order transition in the bulk (1) at H_{CB} followed by the appearance of vortices and a surface state which undergoes a second-order transition at H_{c3} [i.e. (1) II σ].[45,46] Our continuation of the line $\kappa=1/\sqrt{2}$ to the vertex at $\epsilon=\epsilon_{cr}$ is a guess.

Since ϵ and d/λ increase when T decreases, the position of a given film on the graph begins at the left-hand side and moves horizontally to the right when T is lowered. The trajectories would be more complicated if the temperature dependence of κ_1 and κ_2 were used; but our films for $\kappa<0.7$ are not particularly dirty and very precise tests of the theory cannot be made using them.

We have confirmed the diagram by observing experimentally three possible simple trajectories (see Fig. 14):

(a) $\kappa>0.7$: We go from region II S to region (2) II σ at $\epsilon=\epsilon_{cr}$, as shown in Fig. 13.

[43] In order to have a small ϵ and $d/\lambda>\sqrt{5}$, κ must be small. The slope of $J_2(\epsilon)$ curve for $\epsilon=0$ just gives $d=\sqrt{5}\lambda$ for $\kappa=0$.

[44] This is typically the case for pure Pb at 4.2°K.

[45] A similar diagram which has been recently presented by Arp *et al.* (Ref. 46) contains errors because they looked only for one-dimensional solutions of the GL equations and did not consider the vortex studied here.

[46] V. D. Arp, P. S. Collier, R. A. Kamper, and H. Meissner, Phys. Rev. **145**, 231 (1966).

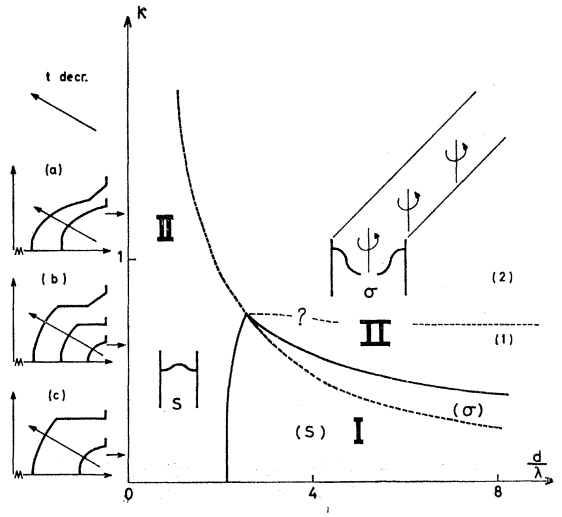

FIG. 14. Nucleation-field diagram for parallel fields. The dotted curve ($d=1.8\ \xi$ or $\epsilon=\epsilon_{cr}$) separates a region to the left which cannot accommodate a vortex structure in high field (state S) and a complementary one which allows vortices (σ). The continuous curve which shows a cusp at $\epsilon=\epsilon_{cr}$ corresponds to the $J_2(\epsilon)$ curve of Fig. 10. Above this curve the high-field transition is second order. Below it, it is first order: then (S) and (σ) refer to supercooling nucleation. This limiting curve is bounded on the left by the value $d/\lambda=\sqrt{5}$, which is the GL result (the larger value of d/λ for larger κ agrees with the result of Arp *et al.*). To the right it goes to $\kappa=0.59$ ($H_{c3}=H_c$). The nearly horizontal line $\kappa=0.7$ is guessed. It separates domains where the transition in the bulk will be first order (1) and second order (2) in lower fields.

We give sets of $D_{V=0}(H)$ curves for three values of κ. (a) gives the same description as Fig. 3. (b) shows the successively obtained first-, second-, and first-order transitions shown more clearly in Fig. 15. (c) is the usual set of curves for pure material (In).

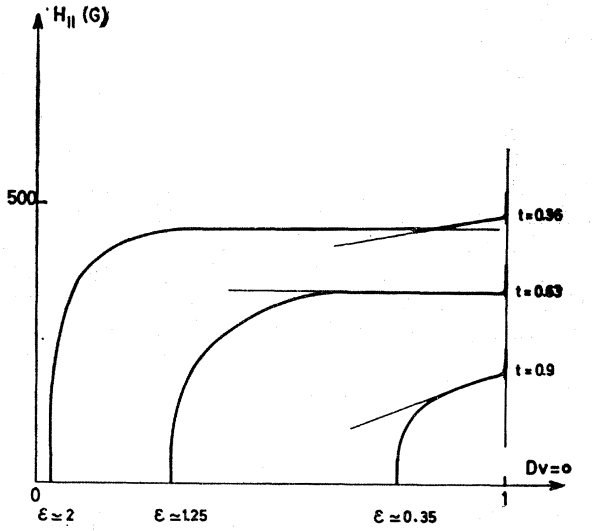

FIG. 15. An experimental set of curves showing the second, first, and second-order transitions of Fig. 14(b). Because of the uncertainty in the $\kappa_{1,2}(t)$ variation, only a qualitative description is possible. However, it seems that the break which occurs just above $t=0.36$ is to be associated with a critical κ_1: The slope after the break is always rather slight, indicating that the nucleation field H_{c3} just crosses the thermodynamic field. We would expect a progressive variation of slope from a very high value if the effect were related to κ_2.

(b) $\kappa<0.4$ (typically for a pure In film): We go from region II S to region I at $d\simeq(\sqrt{5})\lambda$.

(c) $0.4<\kappa<0.7$: The third possibility is clearly displayed in Fig. 15. Near T_c (curve $t=0.9$) we are in region II S characteristic of thin films. When T decreases, we enter region I (curve $t=0.63$) and a first-order transition is seen as in case (b). At the lowest temperatures (curve $t=0.36$) we arrive in region (1) II σ. After the first-order transition at the thermodynamic critical field a state of surface superconductivity appears and persists until H_{c3}, where a second-order transition to the normal state occurs.[47,48] The break in S from the infinite value characteristic of I first appeared for a value $\epsilon_B=1.95>\epsilon_{cr}$.[49] In our expermients on case (c) we have always noted values of $\epsilon_B>\epsilon_{cr}$, and ϵ_B increased when κ of the alloy decreased. This is as expected, as the values of ϵ_B should follow the curve separating region I from region (1) II σ.

Other characteristic trajectories using the variation of κ_1 and κ_2 are possible, but we never observed any of the more complicated transitions predicted by Arp *et al.*[46]

SUMMARY

We have investigated the behavior of alloy films of InBi near the upper critical field H_M for parallel and perpendicular geometries, obtaining values of H_M and of the pair potential [via $|\Delta|^2/(H_M-H)$]. This behavior is well described, with a 5% experimental and theoretical accuracy, if one takes into account the corrections to the formulas applicable to the dirty limit. We have shown that the temperature dependence of the parameter κ_2, related to the value of $|\Delta|^2$, depends on the geometry of the film and field: For thin films in parallel fields with no vortices the original function κ_{2M} calculated by Maki[6] applies, whereas for thick films or for perpendicular geometry the function κ_{2c} found by Caroli *et al.*[9] is appropriate. Intermediate-thickness films in parallel geometry were also studied. They showed very clearly the first entry of vortices in the film when the thickness of the film is large enough [$d>1.8\xi(t)$]; in particular, a discontinuity of $\frac{2}{3}$ in $|\Delta|^2/(H_M-H)$ was observed.

A diagram giving the type of transition to the normal state of fields in parallel geometry as a function of κ and thickness was presented.

Our results can be applied to many studies of the high-field behavior of dirty films which are governed by $|\Delta|^2/(H_M-H)$, such as magnetization[6] and mag-

[47] The same II-I-II trajectory has just been predicted independently by Tilley, Robinson, and Baldwin (Ref. 48).

[48] D. R. Tilley, G. Robinson, and J. P. Baldwin, Mullard Research Laboratory Report No. 2571, 1966 (unpublished).

[49] The ϵ values were determined approximately using the dirty-limit forms.

netic susceptibility, specific heat,[50] attenuation of sound waves,[51] and thermal conductivity.[52]

ACKNOWLEDGMENTS

We are grateful to D. Saint James for writing the program for the numerical calculations and for discussions of surface superconductivity. We acknowledge the help of G. Colliex for the electron-microscope study of our films.

We wish to thank the Orsay group on superconductivity, K. Maki and P. Pincus, for many helpful discussions.

One of us (R.S.T.) wishes to thank C. Bloch and the members of the Service de Physique Théorique for the hospitality accorded him in Saclay.

APPENDIX I: CORRECTIONS DUE TO FINITE l/ξ_0 IN PARALLEL GEOMETRY

In this Appendix we calculate approximately the corrections to the expression (3.3) when l/ξ_0 is finite (the calculation is made for $l/\xi_0 \sim \frac{1}{9}$).[53] The formulas to order A^4 necessary for calculating the critical field have already been studied by one of us [see formula (8), Ref. 29]. Let us summarize the general results.

The expression for ρ of (3.3) becomes

$$\rho f_D/[1+(2n+1)\gamma]^2,$$

where $\gamma=l/\xi_T$, $\xi_T=v_f/2\pi T=0.88\xi_0/t$, and f_D includes effects due to nonlocality and boundary scattering and is a function of $(l/d)1/1+(2n+1)\gamma$.

In *the local limit* $l\ll d$, $f_D=1$; in *the nonlocal limit* $d\ll l$,

$$f_D=(3/8)(d/l)[1+(2n+1)\gamma]. \tag{A1}$$

This changes the form of ρ from H^2d^2 to H^2d^3.

If $\gamma\to 0$, the formulas are just modified by changing d^2 into $d^2 f_D(l/d)$ everywhere.

The fourth-order term contains a factor f' which has the same asymptotic properties as f_D.[54] Thus the fourth-order term is of the same order as the square of the second-order terms only near the local limit. In the nonlocal limit, $f'\gg(f_D)^2$, and the range of convergence of the power series is much restricted.

The density of states was also calculated to second order in A and found to involve only $\rho f_D(l/d)$ in the dirty limit; this is the universal correction to the thickness $f_D d^2$. Corrections of order l/ξ_0 were found to involve not only f_D but a slightly different function g, which is also 1 in the local limit and which becomes $\frac{3}{2}f_D$ in the nonlocal case. Corrections of fourth order in A to the density of states and to the nonlinear term in the GL equation were not evaluated.

Moreover, because of the labor involved in summing very complicated expressions, we will not evaluate the higher-order coefficients exactly, but will instead adopt a *quasilocal approximation*. We will evaluate all the coefficients of the powers of A in the local limit and then multiply each power of A^2 by f_D. Thus we will be taking $f_D{}^2=g^2=f'$. This approximation should be reasonably valid for $l\sim\frac{1}{2}d$ but becomes invalid for $l>d$ at low temperatures. The corrections due to fourth- and higher-order terms in A are about 10%. An error of 50% in the values of the coefficients which give these corrections would give a total correction to 5%, which is tolerable. This approximation is not the same as the local approximation, where spatial variations of the order parameter become very important: We still assume the thin-film limit $d\ll\xi(t)$. However we note that corrections of the same order of magnitude as those calculated here are observed experimentally for the case of not too thin films, which is the basis of the calculation, and for the intermediate and thick-film case.[11] It would be quite difficult to consider the exact form of the corrections in the intermediate range, so we are lucky that the exact form of the coefficients of higher than second order is not too important and that a universal correction is obtained.

The calculation uses the procedure given by Abrikosov and Gor'kov for impurity scattering as applied to thin films by Maki[23]: $i\omega$ and Δ are replaced by

$$\begin{aligned} i\tilde{\omega}&=i\omega-\frac{1}{\tau}\frac{\pi}{mp_f}\int G_\omega(p)\frac{d_3p}{(2\pi)^3},\\ \tilde{\Delta}&=\Delta+\frac{1}{\tau}\frac{\pi}{mp_f}\int F_\omega(p)\frac{d_3p}{(2\pi)^3}\end{aligned} \tag{A2}$$

in the usual equations for F and G. The scattering is assumed isotropic, and τ is the collision transport time.

F and G are expanded to order $|\Delta|^2\Delta$ and $|\Delta|^2$, respectively, in terms of the Green's function of the normal metal, $G(p)=1/(i\omega-\epsilon)$ (the energy $\epsilon=p^2/2m-\epsilon_f$ is measured from the Fermi level). In the presence of a magnetic field, ω is replaced by $\omega+\mathbf{v}\cdot\mathbf{A}$. The integrals of (A2) are evaluated as the residues at the poles $\epsilon=\pm i(\omega+\mathbf{v}\cdot\mathbf{A})$

$$\frac{\pi}{mp_f}\int G_\omega(p)\frac{d_3p}{(2\pi)^3}=1/2-\frac{|\tilde{\Delta}|^2}{4\tilde{\omega}^2}\frac{1}{1+b}, \tag{A3}$$

where $b=(v_FA/\tilde{\omega})^2$,

$$\frac{\pi}{mp_f}\int F_\omega(p)\frac{d_3p}{(2\pi)^3}=\frac{\tilde{\Delta}}{2\tilde{\omega}}\left\{\frac{1}{\sqrt{b}}\tan^{-1}\sqrt{b}-\frac{|\tilde{\Delta}|^2}{4\tilde{\omega}^2}\frac{1}{(1+b)^2}\right\}. \tag{A4}$$

[50] K. Maki, Phys. Rev. **139**, A702 (1965).
[51] M. Cyrot and K. Maki (to be published.)
[52] C. Caroli and M. Cyrot, Phys. Kondenserten Materie 4, 285 (1965).
[53] The actual values for our samples vary slightly around this value. We did not take these variations into account, because they play only a secondary role.
[54] A distinction between specular and diffuse scattering for the higher-order terms (f') is not made in the approximation scheme to follow.

Therefore,

$$\bar{\omega}=\omega+\frac{1}{2\tau}-\frac{1}{2\tau}\frac{|\bar{\Delta}|^2}{2\bar{\omega}^2}\frac{1}{1+b},$$
$$\Delta=\bar{\Delta}\left[1-\frac{1}{2\tau\bar{\omega}}\left\{\frac{1}{\sqrt{b}}\tan^{-1}\sqrt{b}-\frac{|\bar{\Delta}|^2}{2\bar{\omega}^2}\frac{1}{(1+b)^2}\right\}\right]. \quad \text{(A5)}$$

Assuming $\bar{\Delta}$ and Δ constant, we must average these equations over the width of the film at this point. The equation (A5) for Δ is then expanded in powers of $\bar{\Delta}$ and $\bar{\omega}_0=\omega+1/2\tau$:

$$\Delta=\bar{\Delta}\left[1-\frac{1}{2\tau\bar{\omega}}\left\{\left\langle\frac{1}{\sqrt{b}}\tan^{-1}\sqrt{b}\right\rangle+\frac{|\bar{\Delta}|^2}{2\bar{\omega}^2}\left(\frac{1}{2\tau\bar{\omega}}\left\langle\frac{1}{1+b}\right\rangle^2-\left\langle\frac{1}{(1+b)^2}\right\rangle\right)\right\}\right]. \quad \text{(A6)}$$

One may notice that the cancellation $1/2\tau\bar{\omega}-1=\omega/\bar{\omega}$ in the Δ^3 term does not occur to fourth or higher order in **A**. The order parameter is further given as $|\lambda|\pi T\,\Sigma_\omega F(\mathbf{r},\mathbf{r})$, which has already been evaluated to find $\bar{\Delta}$. One finds the GL equation in the usual manner as

$$-\ln t=\sum_{n=0}^{\infty}\left(\frac{1}{n+\frac{1}{2}}-\frac{g}{n+\frac{1}{2}+(1-g)/2\gamma}\right)+\frac{1}{8\pi^2T^2}\Delta^2\frac{\left(n+\frac{1}{2}+\frac{1}{2\gamma}\right)\left\langle\frac{1}{(1+b)^2}\right\rangle-\frac{1}{2\gamma}\left\langle\frac{1}{1+b}\right\rangle^2}{[n+\frac{1}{2}+(1-g)/2\gamma]^4}, \quad \text{(A7)}$$

where

$$\gamma=2\pi\tau T=l/\xi_T,$$
$$g=\langle(1/\sqrt{b})\tan^{-1}\sqrt{b}\rangle=1-\alpha+\beta,$$
$$\alpha=\gamma\rho\frac{1}{[1+(2n+1)\gamma]^2},$$
$$\rho=\frac{\xi_T l}{3}\frac{H^2d^2}{12}f_D$$

as defined before,

$$\beta=(81/25)\alpha^2.$$

The critical field is evaluated by setting $\Delta^2=0$ in (A7), which eliminates the last term. The last term is the expression which reduces to $(\Delta^2/8\pi^2T^2)f_1$ in the dirty limit. The expression which replaces the term $(\frac{1}{2}\rho)\psi_2$ of the dirty limit is found by differentiating the equation for the critical field with respect to H:

$$\frac{\rho}{2}\psi_2\rightarrow\sum_{n=0}^{\infty}\frac{(n+\frac{1}{2}+1/2\gamma)(\alpha-2\beta)}{[n+\frac{1}{2}+(1/2\gamma)(\alpha-\beta)]^2}. \quad \text{(A8)}$$

The correction to the density-of-states factor ψ_3 is found by differentiating the density-of-states correction, which we have evaluated as $\int G_\omega(p)d_3p/(2\pi)^3$, with respect to ω:

$$\frac{d}{d\omega}\frac{\Delta^2}{[\omega+(1/2\tau)(\alpha-\beta)^2]}\left\langle\frac{1}{1+b}\right\rangle. \quad \text{(A9)}$$

Differentiation with respect to ω is of course the same as replacing ω by $\omega+ieV$, differentiating with respect to ieV, and letting V go to zero. Thus we find the corrected factor which goes to ψ_3 in the dirty limit.

$$-\frac{\psi_3}{16}\rightarrow\sum_{n=0}^{\infty}\frac{1}{8}\frac{1-\frac{5\alpha}{1+\gamma(2n+1)}+5\beta+\frac{83}{27}\frac{\beta}{1+\gamma(2n+1)}}{\left[n+\frac{1}{2}+\frac{1}{2\gamma}(\alpha-\beta)\right]^3}. \quad \text{(A10)}$$

These expressions have all been evaluated explicitly by summing the first seven terms in n at four different temperatures: $t\sim0.85$, 0.7, 0.5, and 0.3 with $l/\xi_{T_c}=(2\pi T_c/v_F)l=\frac{1}{8}$. First the value of ρ was found by solving (A7) for the critical field. The theoretical increase of H_M when t decreases was only found to deviate by 1% from the form given by Maki.[6] Thus experimental values should agree with the Maki temperature dependence, as they do. The other corrections found which should multiply the corresponding functions are given in Table II.

TABLE II. Corrections involved in the expression of the slope [Eq. (3.18)] in parallel geometry.

t	Corrected value				
0.848	0.9726 f_1	0.9673 $\rho\psi_2$	0.9753 ψ_3	1.008 $(\psi_3/\rho\psi_2)$	1.019 κ_{2M}
0.696	0.955 f_1	0.949 $\rho\psi_2$	0.9525 ψ_3	1.004 $(\psi_3/\rho\psi_2)$	1.029 κ_{2M}
0.496	0.972 f_1	0.910 $\rho\psi_2$	0.911 ψ_3	1.001 $(\psi_3/\rho\psi_2)$	1.083 κ_{2M}
0.283	0.994 f_1	0.853 $\rho\psi_2$	0.851 ψ_3	0.998 $(\psi_3/\rho\psi_2)$	1.169 κ_{2M}

The corrected values of κ_{2M}/κ are thus 1.004, 0.992, 0.999, 0.998. The calculation is certainly not accurate to 1%: We ignore these small fluctuations and say that κ_2 should be regarded as constant for this case. The same correction in the thick-film limit gives a κ_2 rising twice as fast as in the dirty limit, i.e. as κ_{2c}/κ_{2M}.[55]

Since the correction to $\psi_3/\rho\psi_2$ is always less than 1%, we may say that the correction to the formulas (3.18) for S is just $(\kappa/\kappa_{2M})^{-2}$, which amounts to 0.73 at the lowest temperature ($t=0.3$). However, if we had chosen to express our results in terms of $|\Delta|^2/(H_M-H)$ instead of S, the correction to ψ_3 would have to be employed. It is incorrect to deduce values of $|\Delta|^2/(H_M-H)$ from S by only multiplying by $8\pi^2T^2/\psi_3$ when the dirty limit does not apply. For this reason we prefer to compare the theory directly with the experimentally observable S.

[55] *Note added in proof.* G. Eilenberger (to be published) has recently calculated κ_1 and κ_2 for bulk type-II superconductors for all impurity concentrations. His results are consistent with our assumption about the more rapid increase of $\kappa_2(t)$ than in the dirty limit.

APPENDIX II: DEFINITION OF THE INTEGRALS IN THE NUMERICAL CALCULATION OF S FOR ALL THICKNESSES

First we write L_1, L_2 [Eq. (2.15)], and R (3.10) using Eqs. (3.12) and (3.16) for $\mathbf{j}$ and $|\Delta|^2$:

$$L_1=\frac{D}{2\pi T}\psi_2\int_{-d/2}^{d/2}dx(H_M-H)\int_{-d/2}^{x}dx'\{-Hx'[F^2(x')+F^2(-x')]+k[F^2(x')-F^2(-x')]\}. \tag{B1}$$

The average over y removes the oscillating terms which entered in the definition of L_1, but a contribution from the oscillations remains in L_2 and R owing to the nonvanishing average of $\sin^2 2ky$ when $k\neq 0$:

$$L_2=\left(\frac{D}{2\pi T}\psi_2\right)^2\left(\frac{2v_F^2}{3}\lambda_L^2\right)^{-1}\int_{-d/2}^{+d/2}dx\Bigg[\left\{\int_{-d/2}^{x}dx'(-Hx')[F^2(x')+F^2(-x')]+k[F^2(x')-F^2(-x')]\right\}^2$$
$$+2\left\{\int_{-d/2}^{x}dx'Hx'F^2(x')F^2(-x')\right\}^2\theta_k\Bigg], \tag{B2}$$

where $\theta_k=0$ for $k=0$ and 1 for $k\neq 0$;

$$R=\frac{f_1}{8\pi^2T^2}\int_{-d/2}^{+d/2}dx[\{F^2(x)+F^2(-x)\}^2+2F^2(x)F^2(-x)\theta_k]+\frac{\psi_4}{6}\frac{1}{8\pi^2T^2}\frac{D}{4\pi T}\int_{-d/2}^{+d/2}dx$$
$$\times[\{2F'(x)F(x)-2F'(-x)F(-x)\}^2+2\{F'(x)F(-x)-F(x)F'(-x)\}^2\theta_k+8k^2F^2(x)F^2(-x)], \tag{B3}$$

with

$$\psi_4\left(\frac{1+\rho}{2}\right)=\sum_{n=0}^{\infty}\frac{6}{(n+\frac{1}{2}+\frac{1}{2}\rho)^4},\quad f_1\left(\frac{\rho}{2}\right)=\sum_{n=0}^{\infty}\frac{n+\frac{1}{2}}{(n+\frac{1}{2}+\frac{1}{2}\rho)^4}.$$

R and L have the same $\frac{2}{3}$ discontinuity as the average $\langle|\Delta|^4\rangle$. Hence it is convenient to normalize all the integrals by dividing by $\langle|\Delta|^4\rangle$. We will also remove the temperature-dependent factors in order to define functions only of ϵ. The quantity J_1 also absorbs the value of $|\Delta|^2$ on one of the film boundaries. The arbitrary normalization of F is irrelevant and cancels out thanks to the division by $\langle|\Delta|^4\rangle$:

$$J_1\int_{-d/2}^{+d/2}|\Delta(x)|^4dx=\int_{-d/2}^{+d/2}dx\int_{-d/2}^{x}dx'\{-Hx'[F^2(x')+F^2(-x')]+k[F^2(x')-F^2(-x')]\}[F^2(d/2)+F^2(-\tfrac{1}{2}d)], \tag{B4}$$

$$\tfrac{1}{2}J_2\int_{-d/2}^{+d/2}|\Delta(x)|^4dx=\int_{-d/2}^{+d/2}dx\Bigg[\left\{\int_{-d/2}^{x}dx'(-Hx')[F^2(x')+F^2(-x')]+k[F^2(x')-F^2(-x')]\right\}^2$$
$$+2\left\{\int_{-d/2}^{x}dx'Hx'F^2(x')F^2(-x')\right\}\theta_k\Bigg]. \tag{B5}$$

The first term of R is proportional to $\langle|\Delta|^4\rangle$. We define an integral to measure the strength of the derivatives from the second term of R:

$$C\int_{-d/2}^{+d/2}|\Delta(x)|^4=\xi^2(t)\int_{-d/2}^{+d/2}[\{2F'(x)F(x)-2F'(-x)F(-x)\}^2$$
$$+2\{F'(x)F(-x)-F(x)F'(-x)\}^2\theta_k+8k^2F^2(x)F^2(-x)]. \tag{B6}$$

The results of the numerical calculations are displayed in Figs. 9, 10, and 11.